

# GAIA

## Validation Manual

Version v8p5  
December 1, 2023



# Contents

<b>1</b>	<b>bosse-t2d</b>	<b>7</b>
<b>1.1</b>	<b>Purpose</b>	<b>7</b>
<b>1.2</b>	<b>Description</b>	<b>7</b>
1.2.1	Geometry and Mesh .....	7
1.2.2	Bathymetry .....	7
1.2.3	Initial conditions .....	8
1.2.4	Boundary conditions .....	8
1.2.5	Analytical solution .....	8
1.2.6	Physical parameters .....	9
1.2.7	Numerical parameters .....	9
<b>1.3</b>	<b>Results</b>	<b>9</b>
<b>1.4</b>	<b>Conclusion</b>	<b>10</b>
<b>2</b>	<b>bosse-t3d</b>	<b>11</b>
<b>2.1</b>	<b>Purpose</b>	<b>11</b>
<b>2.2</b>	<b>Description</b>	<b>11</b>
2.2.1	Geometry and mesh discretization .....	11
2.2.2	Bathymetry .....	11
2.2.3	Initial conditions .....	12
2.2.4	Boundary conditions .....	12
2.2.5	Physical and numerical parameters .....	12
<b>2.3</b>	<b>Results</b>	<b>12</b>
<b>2.4</b>	<b>Conclusion</b>	<b>13</b>
<b>3</b>	<b>bump2d</b>	<b>14</b>
<b>3.1</b>	<b>Purpose</b>	<b>14</b>
<b>3.2</b>	<b>Description of the problem</b>	<b>14</b>
3.2.1	Reference .....	14
3.2.2	Physical parameters .....	14
3.2.3	Geometry and Mesh .....	15
3.2.4	Initial and Boundary Conditions .....	15
3.2.5	Numerical parameters .....	15

<b>3.3</b>	<b>Results</b>	<b>16</b>
<b>4</b>	<b>Cohesive channel . . . . .</b>	<b>17</b>
<b>4.1</b>	<b>Erosion</b>	<b>17</b>
4.1.1	Purpose . . . . .	17
4.1.2	Description . . . . .	17
4.1.3	Physical parameters . . . . .	17
4.1.4	Analytical solution . . . . .	18
4.1.5	Numerical parameters . . . . .	18
4.1.6	Results . . . . .	18
4.1.7	Conclusion . . . . .	18
<b>4.2</b>	<b>Deposition</b>	<b>19</b>
4.2.1	Purpose . . . . .	19
4.2.2	Description . . . . .	19
4.2.3	Physical parameters . . . . .	19
4.2.4	Analytical solution . . . . .	20
4.2.5	Numerical parameters . . . . .	21
4.2.6	Results . . . . .	21
4.2.7	Conclusion . . . . .	21
<b>5</b>	<b>Continuous Vertical Sorting Model . . . . .</b>	<b>23</b>
<b>5.1</b>	<b>Purpose</b>	<b>23</b>
<b>5.2</b>	<b>Problem setup</b>	<b>23</b>
<b>5.3</b>	<b>Numerical setup</b>	<b>24</b>
<b>5.4</b>	<b>Results</b>	<b>25</b>
<b>5.5</b>	<b>References</b>	<b>25</b>
<b>6</b>	<b>flume_bc . . . . .</b>	<b>29</b>
<b>6.1</b>	<b>Purpose</b>	<b>29</b>
<b>6.2</b>	<b>Description</b>	<b>29</b>
<b>6.3</b>	<b>Physical parameters</b>	<b>29</b>
6.3.1	Geometry and Mesh . . . . .	29
<b>6.4</b>	<b>Initial and Boundary Conditions</b>	<b>30</b>
6.4.1	Initial conditions . . . . .	30
6.4.2	Boundary conditions . . . . .	30
<b>6.5</b>	<b>Numerical parameters</b>	<b>30</b>
<b>6.6</b>	<b>Results</b>	<b>30</b>
6.6.1	Case 1 . . . . .	30
6.6.2	Case 2 . . . . .	31
6.6.3	Case 3 . . . . .	32
6.6.4	Case 4 . . . . .	32
6.6.5	Case 5 . . . . .	32
6.6.6	Case 6 . . . . .	33
<b>6.7</b>	<b>Conclusion</b>	<b>33</b>

<b>7</b>	<b>guenter-t2d</b>	<b>34</b>
7.1	Purpose	34
7.2	Description	34
7.3	Physical parameters	34
7.3.1	Geometry and Mesh	35
7.4	Initial and Boundary Conditions	35
7.4.1	Initial conditions	35
7.4.2	Boundary conditions	35
7.5	Numerical parameters	35
7.6	Results	35
7.7	Conclusion	39
<b>8</b>	<b>hippodrome-t2d</b>	<b>40</b>
8.1	Purpose	40
8.2	Description	40
8.2.1	Geometry, initial bathymetry and mesh discretization	40
8.2.2	Bathymetry	41
8.2.3	Initial conditions	41
8.2.4	Boundary conditions	41
8.2.5	Physical and numerical parameters	41
8.3	Results	41
8.4	Conclusion	42
<b>9</b>	<b>Littoral</b>	<b>43</b>
9.1	Purpose	43
9.2	Description of the problem	43
9.3	Physical parameters	43
9.3.1	Geometry and Mesh	43
9.4	Initial and Boundary Conditions	43
9.4.1	Wave conditions	43
9.5	Numerical parameters	43
9.6	Results	44
9.7	A new way to couple telemac2d and tomawac	45
9.7.1	Results using the same mesh	46
9.7.2	Results using different meshes	47
<b>10</b>	<b>lyn-t3d</b>	<b>50</b>
<b>11</b>	<b>Conservation (mud_conservation-t2d)</b>	<b>51</b>
11.1	Purpose	51

<b>11.2 Description</b>	<b>51</b>
11.2.1 Geometry and Mesh . . . . .	51
11.2.2 Initial conditions . . . . .	52
11.2.3 Boundary conditions . . . . .	52
11.2.4 Physical parameters . . . . .	52
11.2.5 Numerical parameters . . . . .	52
<b>11.3 Results</b>	<b>52</b>
<b>11.4 Conclusion</b>	<b>53</b>
<b>12 rouse-t3d . . . . .</b>	<b>54</b>
<b>12.1 Purpose</b>	<b>54</b>
<b>12.2 Description</b>	<b>54</b>
12.2.1 Geometry and Mesh . . . . .	54
12.2.2 Physical parameters . . . . .	55
12.2.3 Initial and Boundary Conditions . . . . .	55
12.2.4 General parameters . . . . .	56
12.2.5 Numerical parameters . . . . .	56
12.2.6 Comments . . . . .	56
<b>12.3 Results</b>	<b>56</b>
<b>12.4 Conclusion</b>	<b>56</b>
12.4.1 Reference . . . . .	57
<b>13 Sliding . . . . .</b>	<b>58</b>
<b>13.1 Purpose</b>	<b>58</b>
<b>13.2 Problem setup</b>	<b>58</b>
<b>13.3 Numerical setup</b>	<b>58</b>
<b>13.4 Results</b>	<b>59</b>
<b>14 Tidal_flats-t3d . . . . .</b>	<b>62</b>
<b>14.1 Purpose</b>	<b>62</b>
<b>14.2 Description</b>	<b>62</b>
14.2.1 Geometry . . . . .	62
14.2.2 Physical parameters . . . . .	63
14.2.3 Initial and Boundary Conditions . . . . .	63
14.2.4 General parameters . . . . .	64
14.2.5 Numerical parameters . . . . .	64
<b>14.3 Results</b>	<b>64</b>
<b>14.4 Conclusion</b>	<b>65</b>
14.4.1 Reference . . . . .	65
<b>15 Turbidity channel . . . . .</b>	<b>67</b>
<b>15.1 Purpose</b>	<b>67</b>

<b>15.2</b>	<b>Problem setup</b>	<b>67</b>
<b>15.3</b>	<b>Numerical setup</b>	<b>68</b>
<b>15.4</b>	<b>Results</b>	<b>68</b>
15.4.1	Plunging point . . . . .	68
<b>15.5</b>	<b>Reference</b>	<b>69</b>
<b>16</b>	<b>WC_BOMC4: experiments of Wilcock and Crowe (2003) . . . . .</b>	<b>70</b>
<b>16.1</b>	<b>Validation with the experiments of WC-2003</b>	<b>70</b>
<b>16.2</b>	<b>Implementation of sediment recirculation</b>	<b>70</b>
16.2.1	Implementation of sediment recirculation in Sisyphe (not in library) . . . . .	71
<b>17</b>	<b>Yen . . . . .</b>	<b>73</b>
<b>17.1</b>	<b>Purpose</b>	<b>73</b>
<b>17.2</b>	<b>Problem setup</b>	<b>73</b>
<b>17.3</b>	<b>Numerical setup</b>	<b>74</b>
<b>17.4</b>	<b>Results</b>	<b>74</b>
<b>17.5</b>	<b>References</b>	<b>75</b>
	<b>Bibliography . . . . .</b>	<b>78</b>

# 1. bosse-t2d

## 1.1 Purpose

The capabilities of the morphodynamics module at reproducing the evolution of an initially symmetric, isolated bedform subject to unidirectional flow is considered in this test case. The test is useful to check that the bedform propagates with the right celerity on one hand and that the numerical schemes can handle shock formation on the other hand.

## 1.2 Description

### 1.2.1 Geometry and Mesh

The channel is 16m long and 1m width. The computational domain is discretized with irregular triangular elements with an average size equal to 0.2 m. It is made up by 534 nodes and 896 elements (cf. figure 1.1).

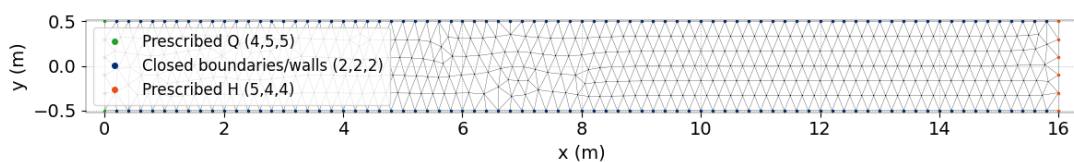


Figure 1.1: Geometry and mesh of bosse-t2d test case.

### 1.2.2 Bathymetry

The bottom is flat with a finite amplitude perturbation of the bed level (see figure 1.2) given by equation:

$$z_b = \begin{cases} 0.1 \sin^2 \left( \frac{\pi(x-2)}{8} \right), & \text{si } 2m \leq x \leq 10m \\ 0, & \text{otherwise} \end{cases} \quad (1.1)$$

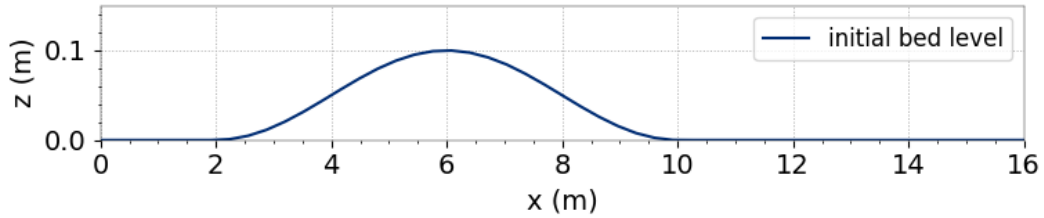


Figure 1.2: 1D profile of initial bed level.

### 1.2.3 Initial conditions

The velocity field is set to zero and the water surface elevation is set to 0.6 m.

### 1.2.4 Boundary conditions

At the left boundary we set a discharge equal to  $0.25 \text{ m}^3 \text{s}^{-1}$  and an equilibrium sediment discharge. At the right boundary, the water surface elevation is set to 0.6 m and a free condition is set for sediments.

Lateral boundaries are considered as solid walls without friction.

### 1.2.5 Analytical solution

The sediment transport capacity ( $q_s$ ) can be expressed as  $q_s = AV^m$  (see Kubatko and Westerink [10]) with  $A$  and  $m$  constants and  $V$  the average fluid velocity ( $\text{m s}^{-1}$ ), assuming the unit fluid discharge as constant  $q$  ( $\text{m}^2 \text{s}^{-1}$ ). The Exner equation can then be written as:

$$\frac{\partial z_b}{\partial t} + \frac{1}{1-\lambda} \frac{\partial}{\partial x} A \left( \frac{q}{Z_s - z_b} \right)^m = 0. \quad (1.2)$$

with  $z_b$  the bed elevation (m),  $\lambda$  the porosity (/), and  $Z_s$  the free surface elevation (m).

We rewrite the above equation as:

$$\frac{\partial z_b}{\partial t} + \frac{1}{1-\lambda} \frac{\partial}{\partial z_b} A \left( \frac{q}{Z_s - z_b} \right)^m \frac{\partial z_b}{\partial x} = 0$$

that is:

$$\frac{\partial z_b}{\partial t} + \frac{1}{1-\lambda} \left( \frac{Amq^m}{(Z_s - z_b)^{m+1}} \right) \frac{\partial z_b}{\partial x} = 0$$

also written as:

$$\frac{\partial z_b}{\partial t} + c(z_b) \frac{\partial z_b}{\partial x} = 0 \quad (1.3)$$

with  $c(z_b)$  the bed celerity, or propagation speed of the bed, ( $\text{m s}^{-1}$ ), expressed by:

$$c(z_b) = \frac{1}{1-\lambda} \frac{mAq^m}{(Z_s - z_b)^{m+1}} \quad (1.4)$$

Giving an initial condition  $z_b(x, 0) = z_{b,0}(x)$ , the equation (1.3) has the following exact solution :

$$z_b(x, t) = z_b(x, 0)(x - c(z_b)t) \quad (1.5)$$

till the time of wave breaking (i.e. shock formation), see also Kubatko and Westerink [10]:

$$t = - \frac{1}{\min_{-2 \leq x \leq 10} (F'(x))} \quad (1.6)$$

with  $F(x) = c(z_b(x, t = 0))$ .

We choose to express the solid discharge with the Engelund-Hansen formula:

$$q_s = 0.1 \left[ (s - 1) g d^3 \right]^{1/2} \frac{\theta^{5/2}}{c_f}$$

with  $c_f$  the adimensional friction coefficient,  $\theta$  the Shields number ( $\theta = \frac{\tau_b}{(\rho_s - \rho)gd}$ ) and  $s$  the relative density of sediment. By explicitation of the Shields number, we obtain:

$$q_s = \frac{0.1}{c_f} \left[ (s - 1) g d^3 \right]^{1/2} \left( \frac{1}{2} \frac{c_f}{(s - 1)g d} \right)^{5/2} ||\mathbf{u}||^5$$

Then, the parameters to compute the bed celerity are:

$$A = \frac{0.1}{c_f} \left[ (s - 1) g d^3 \right]^{1/2} \left[ \frac{c_f}{2g(s-1)d} \right]^{5/2} \text{ and } m = 5.$$

### 1.2.6 Physical parameters

The bottom friction is described by the Stricker law, with a coefficient equal to  $50 \text{ m}^{1/3}\text{s}^{-1}$ . The turbulence is modelled by a constant viscosity law with a diffusion coefficient equal to  $\nu = 10^{-6} \text{ m}^2\text{s}^{-1}$ .

The bed is composed of sediments with a constant median diameter  $d_m = 0.15 \text{ mm}$  and a porosity equal to 0.375.

### 1.2.7 Numerical parameters

The time step is set to  $\Delta t = 0.1 \text{ s}$  and the duration is equal to 35000 s. The sediment transport capacity is computed with the Engelund and Hansen formula. Bedload is modeled with two different schemes:

- a finite element method (default option)
- an upwind finite volume method

Note that to choose an upwind finite volume method, user must use **FINITE VOLUMES** = YES and **UPWINDING FOR BEDLOAD** = 1.

## 1.3 Results

The results obtained for the two schemes are compared to the exact solution computed with the method of characteristics. Comparisons are shown at two different times in figure 1.3.

The figure on the left shows the solution before shock formation. In this case, numerical results show that the bedform moves with the same celerity for finite element and finite volume scheme, which is slightly faster than the one given by the exact solution. The figure on the right shows the solution once shock appears. In this case the finite element scheme shows some oscillations, while finite volume scheme presents a smooth solution.

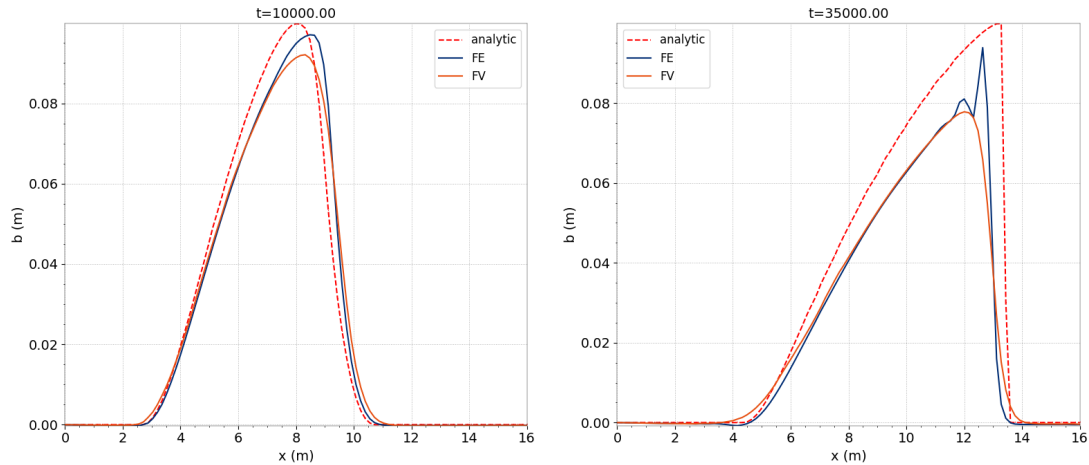


Figure 1.3: Bed elevation: comparison between numerical solutions and exact solution computed with characteristics method at different times.

## 1.4 Conclusion

This test shows that GAIA can reproduce the evolution of a bedform, subject to unidirectional flow, capturing shocks formation.

## 2. bosse-t3d

### 2.1 Purpose

The simulation of the propagation of an initially symmetric bump in a three-dimensional flow field is proposed in this test case. As for the case *bosse-t2d*, this case assesses the capability of the model at propagating an isolated bedform subject to a unidirectional hydrodynamic forcing.

### 2.2 Description

#### 2.2.1 Geometry and mesh discretization

The computational domain consists of a rectangular flume with dimensions 16m long times 1m wide, discretized with 1600 triangular elements, see figure 2.1. The three-dimensional discretization is obtained by first dividing the two-dimensional domain with non-overlapping linear triangles and followed by extruding each triangle along the vertical direction into linear prismatic columns that exactly fitted the bottom and the free surface. Then, each column is partitioned into non-overlapping layers. For this test case, 15 superimposed layers are used along the vertical direction.

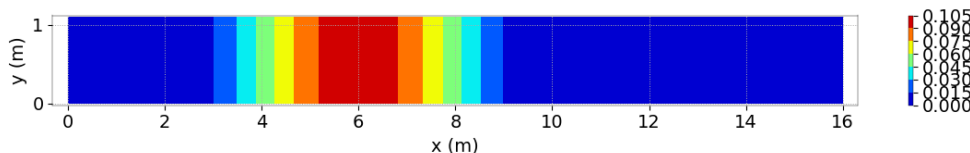


Figure 2.1: Mesh discretization and bathymetry of the *bosse-t3d* test case.

#### 2.2.2 Bathymetry

As for the *bosse-t2d* case, the bottom is flat with a finite amplitude perturbation of the bed level (see figure 2.2) given by equation:

$$z_b = \begin{cases} 0.1 \sin^2 \left( \frac{\pi(x-2)}{8} \right), & \text{si } 2\text{m} \leq x \leq 10\text{m} \\ 0, & \text{otherwise} \end{cases} \quad (2.1)$$

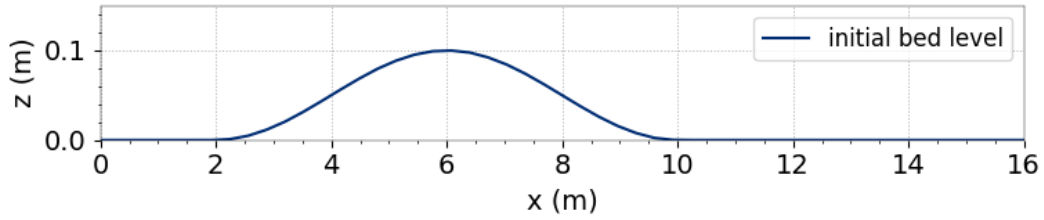


Figure 2.2: 1D profile of initial bed level.

### 2.2.3 Initial conditions

The hotstart file `bosse-t2d_init` computed from a TELEMAC-2D simulation provides the initial conditions for the velocity field and water-depth over the computational domain.

### 2.2.4 Boundary conditions

At the left boundary we set a discharge equal to  $0.25 \text{ m}^3\text{s}^{-1}$  and an equilibrium sediment discharge. At the right boundary, the water surface elevation is set to 0.6 m and a free boundary condition is set for sediments. Lateral boundaries are considered as solid walls without friction.

### 2.2.5 Physical and numerical parameters

The bottom friction is described by the Stricker law, with a coefficient equal to  $50 \text{ m}^{1/3}\text{s}^{-1}$ . The horizontal turbulence is modelled by a constant viscosity model with a horizontal diffusion coefficient equal to  $v_h = 10^{-1} \text{ m}^2\text{s}^{-1}$ . The vertical turbulence is parameterized with a mixing-length model with a vertical diffusion coefficient equal to  $v_v = 10^{-6} \text{ m}^2\text{s}^{-1}$ .

The bed is composed of sediments with a constant median diameter  $d_m = 0.15 \text{ mm}$  and a porosity equal to 0.375. The sediment transport mechanism considered for this test case is bedload. The sediment transport capacity is computed with the (total) Engelund and Hansen parameterization formula.

The time step is set to  $\Delta t = 1 \text{ s}$  and the duration is equal to 14000 s.

## 2.3 Results

Figure 2.3 shows the evolution of the bedform at times 3000s, 6000s, 9000s and 12000s. The bump exhibits the characteristics behaviour of propagating sand-wave that evolves and start developing a shock wave, without decreasing of its amplitude.

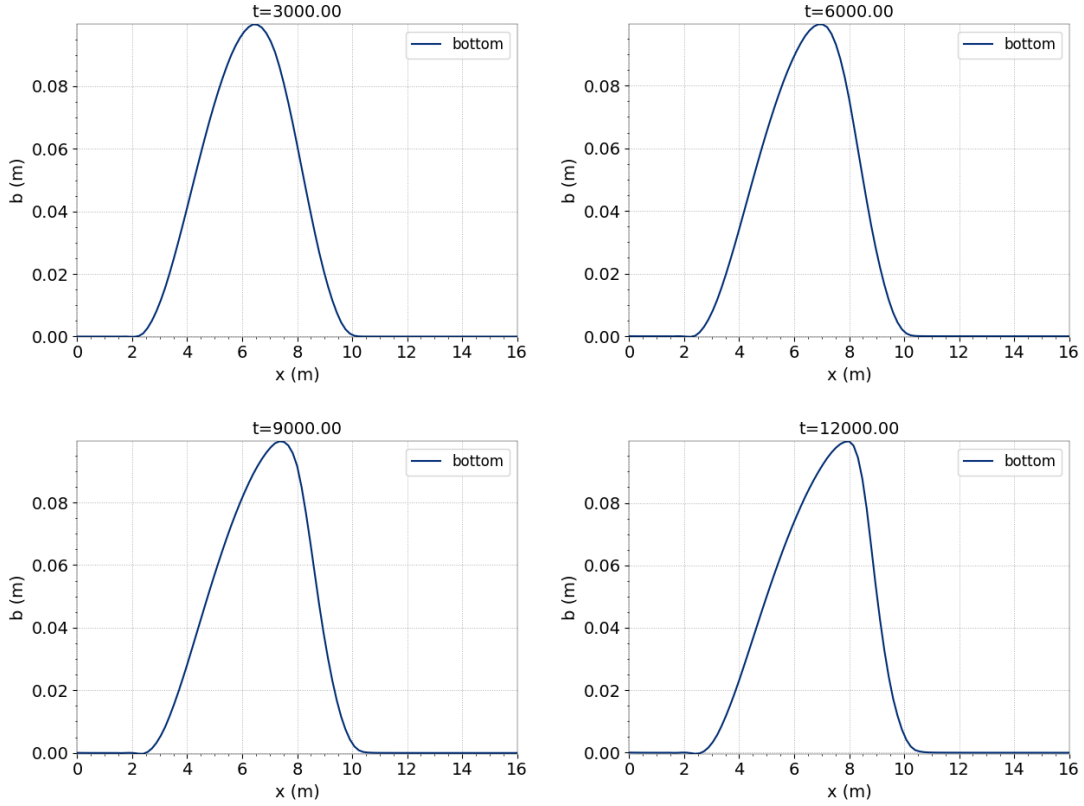


Figure 2.3: Bed evolution at times 3000s, 6000s, 9000s and 12000s.

## 2.4 Conclusion

This test shows that GAIA is able to reproduce the propagation of an isolated bedform, subject to a unidirectional flow in a three-dimensional domain.

## 3. bump2d

### 3.1 Purpose

The evolution of a conical dune is commonly used as a test case for two dimensional morphodynamic models. The flow is almost uniform and sub-critical. This test case was proposed by Hudson (2005). De Vriend (1987) obtained an approximate analytical solution for the spread angle.

### 3.2 Description of the problem

The sediment dune propagates downstream during the simulation. The formerly conical dune evolves towards a star-shaped pattern expanding in time with a fixed spread angle.

#### 3.2.1 Reference

- De Vriend, H.J. *2DH mathematical modelling of morphological evolutions in shallow water*. Coastal Engineering, 11(1):1 – 27, 1987.
- Grass, A.J. *Sediment transport by waves and currents*. Technical Report FL29, SERC London Centre for Marine Technology, 1981.
- Hudson, J. and Sweby, P.K. *A high-resolution scheme for the equations governing 2D bed-load sediment transport*. International Journal for Numerical Methods in Fluids, 47:1085–1091, 2005.
- Siviglia, A., Stecca, G., Vanzo, Zolezzi, G., Toro, E.F., Tubino, M. *Numerical modelling of two-dimensional morphodynamics with applications to river bars and bifurcations*. Advances in Water Resources, February 2013. DOI:10.1016/j.advwatres.2012.11.010

#### 3.2.2 Physical parameters

The bed load transport  $QS$  is calculated with the velocities  $u$  and  $v$  using the total load formula of Grass (1981). There are two parameters in the formula: the constant  $A_G [s^2/m]$  and the exponent  $m_g$ . The first is usually obtained by experimental data and takes into account the grain diameter and the cinematic viscosity. It is set to  $0.00167 m^2/s$  for the simulation. The second parameter is as here usually set to  $m_g = 3$ . The following formula is implemented in the subroutine qsform.f:

$$\begin{aligned} QS &= A_G = u|u|^{(m_g-1)} \\ QS &= A_G(u^2 + v^2)\sqrt{u^2 + v^2} \end{aligned} \tag{3.1}$$

No bottom friction, no diffusion, no porosity and no slope effect is included in the simulation.

### 3.2.3 Geometry and Mesh

The problem is solved in the square computational domain  $[0; 1000] \times [-500; 500]$  m using an unstructured triangle grid with 2601 nodes and 5000 elements (see figure 3.1).

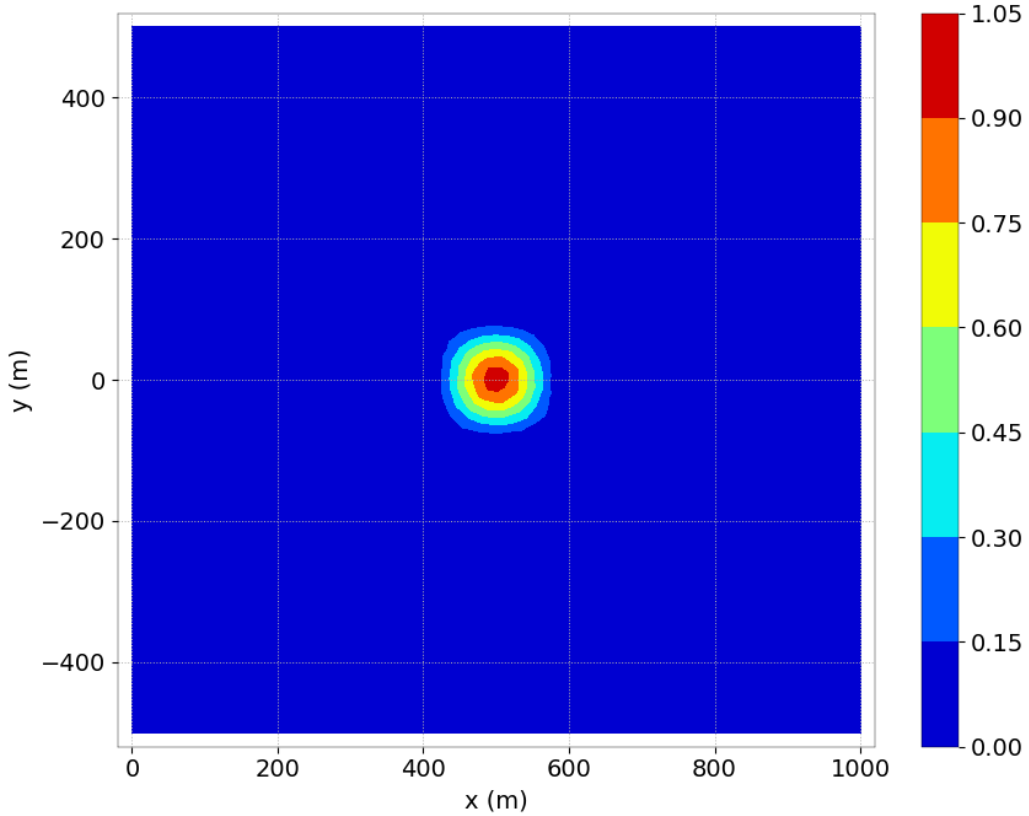


Figure 3.1: Simulation grid and initial bottom

### 3.2.4 Initial and Boundary Conditions

The initial condition for the bed elevation  $z$  is given by flat horizontal bed with a sediment bump:

$$z(x, y) = \begin{cases} \sin^2\left(\frac{\pi(x-400)}{200}\right) \sin^2\left(\frac{\pi(y+100)}{200}\right) & \text{if } x \in [400, 600] \\ 0 & \text{and } y \in [-100, 100] \\ 0 & \text{otherwise} \end{cases} \quad (3.2)$$

The initial condition for the hydrodynamic is the steady state computed with the following boundary conditions. At the upstream boundary  $x = 0$  a constant discharge of  $Q = 1000 \text{m}^3/\text{s}$  is prescribed while a free outflow condition with a fixed water level of 10 m is set at the downstream boundary  $x = 1000$  m. At the side boundaries  $y = -500$  and  $y = 500$  m a slip condition is imposed. For the morphodynamic simulation only bed load transport is taken into account. There is no sediment input to the boundaries.

### 3.2.5 Numerical parameters

The time step is set to 2 s and the simulation is coupled with GAIA.

### 3.3 Results

The analytical solution for the spread angle  $\alpha^s$

$$\alpha^s = \arctan\left(\frac{3\sqrt{3}(m_G - 1)}{9m_G - 1}\right) \quad (3.3)$$

is valid under the hypothesis of weak interaction between sediment layer and fluid, which is ensured setting  $A_G = 0.00167 < 0.01$  in the Grass formula. With this parameters the spread angle of the analytical solution is  $\alpha^s = 21.787$ .

The spread angle from the simulation is calculated by using the 0.1 m bottom isolines after 80 h and 100h simulation time (see figure 3.2).

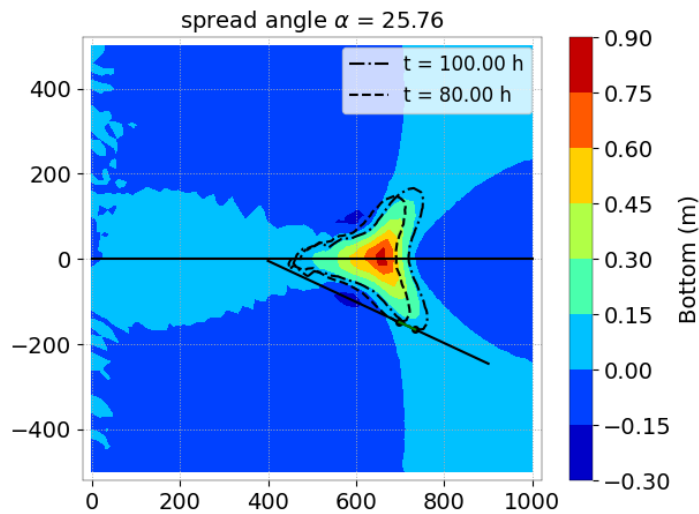


Figure 3.2: Simulation results after 100h

## 4. Cohesive channel

### 4.1 Erosion

#### 4.1.1 Purpose

The purpose of this test case is to validate the calculation of the erosion flux and the evolution of the suspended sediment concentration along the channel.

#### 4.1.2 Description

To obtain an analytical solution, the bathymetry evolution is not updated due to erosion (bottom artificially fixed by a high density). We are interested in the erosion of the bottom in a rectangular channel. Friction is considered to be zero on the bottom and on the walls.

#### 4.1.3 Physical parameters

The river is a rectangular channel with flat bottom, length  $L$ , width  $La$ , zero slope.

Table 4.1: Parameters of test case: erosion in a rectangular channel

$L$	1500	m	Length of the channel
$La$	50	m	Width of the channel
$M$	$10^{-2}$	$\text{kg m}^{-2} \text{s}^{-1}$	Partheniades constant
$\tau_{ce}$	0.01	Pa	Critical erosion stress
$C_0$	0	g/l	Concentration entering the channel
$Q$	50	$\text{m}^3 \text{s}^{-1}$	Flow rate into the channel
$H$	4.5	m	Water depth downstream
$K_p$	85	$\text{m}^{1/3} \text{s}^{-1}$	Skin Strickler coefficient

We consider the flow initially as uniform and permanent with an initial concentration of zero sediment. The skin Strickler coefficient is directly set via the user fortran file in the shear stress formula.

Being in river flow, we impose two boundary conditions:

- upstream, a constant flow  $Q$  and concentration  $C_0$ ;
- downstream, a constant elevation and a free sediment flow.

To highlight erosion, additional assumptions must be made: Deposition must be zero, therefore the settling velocity of the mud will be zero, and the critical deposition shear stress is set to a value never reached.

#### 4.1.4 Analytical solution

The equation to solve is:

$$U \frac{\partial C}{\partial x} - k_x \frac{\partial^2 C}{\partial x^2} = \frac{\Phi_{erosion}}{A}, \quad (4.1)$$

with as boundary conditions  $C(x=0) = C_0$  and  $\left(\frac{\partial C}{\partial x}\right)_{x=L} = 0$ , with  $H$ , the water depth, and the erosion flux according to Partheniades law, the equation (4.1) becomes:

$$U \frac{\partial C}{\partial x} - k_x \frac{\partial^2 C}{\partial x^2} = \frac{M(\tau/\tau_{ce} - 1)}{H}. \quad (4.2)$$

In **the case where the diffusion is zero**,  $k_x = 0$ , and the equation (4.2) turns into a simple first-order differential equation, whose solution is:

$$C(x) = \alpha \frac{x}{L} + C_0, \quad (4.3)$$

where  $\alpha = \frac{LM(\tau/\tau_{ce}-1)}{UH}$ , where  $\tau = \rho g H(x,y) J = \frac{\rho g H(x,y) u^2}{K_p^2 R_h^{4/3}}$

If **the scattering is not zero**,  $k_x \neq 0$ , the equation (4.2) is rewritten in terms of the Peclet number,  $Pe = \frac{UL}{k_x}$ , and  $\alpha$ . The Peclet number represents the ratio of convection to diffusion. The equation is then written:

$$\frac{1}{Pe} \frac{\partial^2 C}{\partial x^2} - \frac{1}{L} \frac{\partial C}{\partial x} = -\frac{\alpha}{L^2}, \quad (4.4)$$

whose solution can be written:

$$C(x) = C_0 + \alpha \frac{x}{L} + \frac{\alpha}{Pe} \left( e^{-Pe} - e^{-Pe(1-x/L)} \right). \quad (4.5)$$

We study the results of this test case for two different values of Peclet number : an infinite Peclet number (there is no diffusion) and a Peclet number of 1 (the diffusion is as important as the convection). The corresponding diffusion coefficients are 0 and 333.3 m<sup>2</sup>/s.

For a Peclet equal to 1, diffusion has the effect of decreasing the concentration of SS from the first meters of the reach, and consequently the concentration at the end of the channel is three times lower than the case without diffusion.

#### 4.1.5 Numerical parameters

The duration is set to 30 000 s and the time step is 1 s. The mesh size is 10 m.

#### 4.1.6 Results

Figure 4.1 and 4.2 show the suspended sediment concentration along the channel simulated, in comparison with the analytical solution.

#### 4.1.7 Conclusion

The erosion flux is well represented.

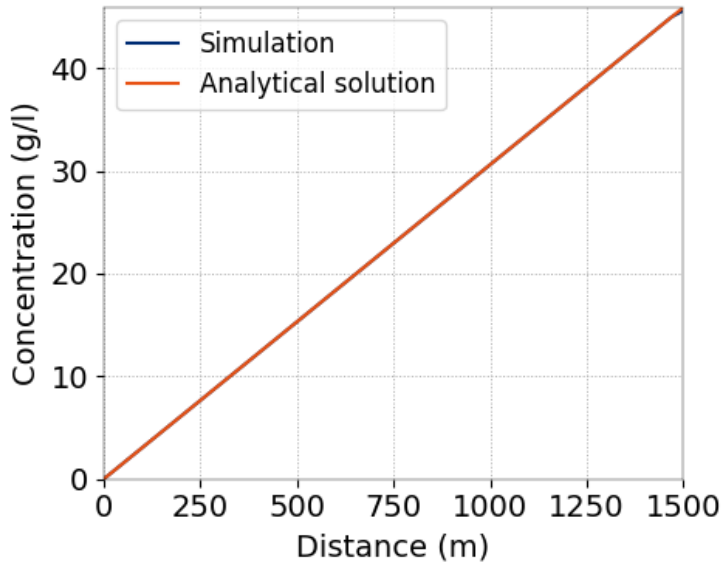


Figure 4.1: Concentration along the channel without diffusion, simulation vs analytical solution.

## 4.2 Deposition

### 4.2.1 Purpose

The purpose of this test case is to validate the calculation of the deposition flux and the evolution of the suspended sediment load concentration along the channel.

### 4.2.2 Description

In order to obtain an analytical solution, the bathymetry evolution is not updated after the deposition (bottom artificially fixed by setting a high density of sediment). We are interested in a deposition phenomenon with entry of SS in the channel. Friction is considered to be nil on the bottom and on the walls.

### 4.2.3 Physical parameters

One considers a rectangular channel with flat bottom, of length  $L$ , width  $La$ , and zero slope.

$L$	1500	m	Length of the channel
$La$	50	m	Width of the channel
$ws$	$1.5 \cdot 10^{-4}$	m/s	Settling velocity of the mud
$\tau_{cd}$	0.1	Pa	Critical deposition shear stress
$C_0$	1	g/l	Inflow concentration
$Q$	10	$\text{m}^3 \text{s}^{-1}$	Channel discharge
$H$	4.5	m	Water depth
$K_p$	85	$\text{m}^{1/3} \text{s}^{-1}$	Skin friction coefficient

Table 4.2: Parameters of deposition test case.

Being in fluvial flow, one imposes two boundary conditions:

- upstream, a constant flow and concentration  $Q$  and  $C_0$ ;

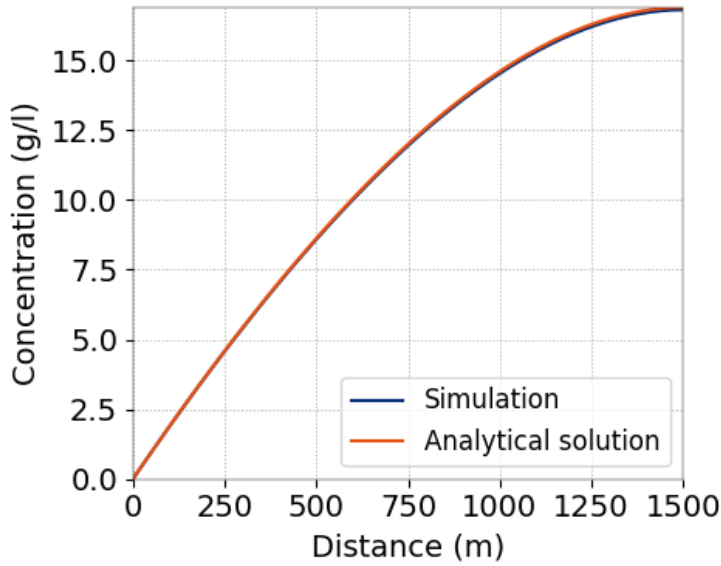


Figure 4.2: Concentration along the channel with diffusion, simulation vs analytical solution.

- downstream, a constant elevation and a free sediment flow.

Since we will be highlighting deposition, additional assumptions must be made:

- the erosion must be null, that is why the coefficient of Parthéniades will be taken null;
- we study an established regime, to obtain the update of the geometry of the bottom of the channel following the deposit is not carried out.

#### 4.2.4 Analytical solution

Under these assumptions and this geometry, the equation to be treated becomes:

$$U \frac{\partial C}{\partial x} - k_x \frac{\partial^2 C}{\partial x^2}, = \frac{\Phi_{depot}}{A} \quad (4.6)$$

with the boundary conditions defined as  $C(x = 0) = C_0$  and  $\left(\frac{\partial C}{\partial x}\right)_{x=L} = 0$ , with  $H$  the water depth, and the deposition flux given by the Krone law, equation (4.6) becomes :

$$U \frac{\partial C}{\partial x} - k_x \frac{\partial^2 C}{\partial x^2}, = \frac{Cw_s(1 - \tau/\tau_{cd})}{H} \quad (4.7)$$

Under the assumptions of non-variation of the geometry, this differential equation has an analytical solution because these coefficients are constant.

In the case of zero diffusion,  $k_x = 0$ , the equation (4.6) turns into a simple first order differential equation:

$$\frac{\partial C}{\partial x} = -\frac{\alpha}{L} C, \quad (4.8)$$

where  $\alpha = \frac{Lw_s(1 - \tau/\tau_{cd})}{UH}$ .

donc la solution est :

$$C(x) = C_0 e^{-\alpha x/L}. \quad (4.9)$$

If  $k_x \neq 0$ , the equation (4.6) is written depending on the Peclet number,  $Pe = \frac{UL}{k_x}$ , and on  $\alpha$ :

$$\frac{1}{Pe} \frac{\partial^2 C}{\partial x^2} - \frac{1}{L} \frac{\partial C}{\partial x} = -\frac{\alpha}{L^2}, \quad (4.10)$$

then the solution writes:

$$C(x) = \frac{\omega_2 e^{\omega_2 x/L} - \omega_1 e^{\omega_1 x/L}}{\omega_2 e^{\omega_2} - \omega_1 e^{\omega_1}}, \quad (4.11)$$

with

$$\omega_1 = \frac{1 + \sqrt{1 + 4\alpha/Pe}}{2/Pe}, \quad (4.12)$$

$$\omega_2 = \frac{1 - \sqrt{1 + 4\alpha/Pe}}{2/Pe}. \quad (4.13)$$

As for erosion, the phenomenon of diffusion is introduced with a Peclet number of 1 (with a value of diffusion coefficient equal to  $75 \text{ m}^2/\text{s}$ ), an infinite Peclet number is also tested ( $k_x = 0 \text{ m}^2/\text{s}$ ).

#### 4.2.5 Numerical parameters

The duration is set to 80 000 s and the time step is 1 s. The mesh size is 10 m.

#### 4.2.6 Results

Figure 4.3 and 4.4 show the suspended sediment concentration along the channel simulated, in comparison with the analytical solution.

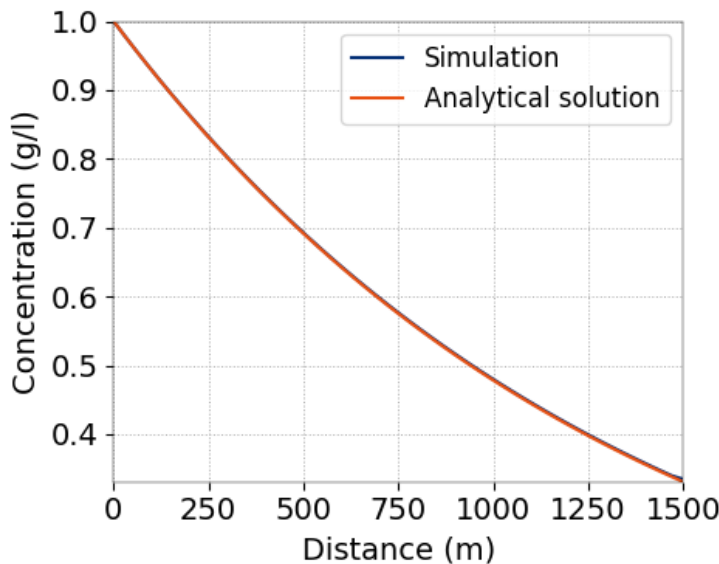


Figure 4.3: Concentration along the channel without diffusion, simulation vs analytical solution.

#### 4.2.7 Conclusion

The deposition flux is well represented.

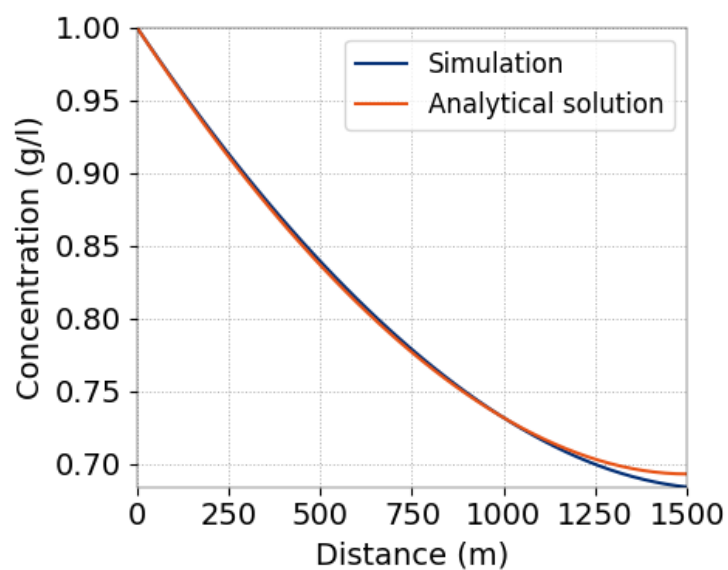


Figure 4.4: Concentration along the channel with diffusion, simulation vs analytical solution.

## 5. Continuous Vertical Sorting Model

### 5.1 Purpose

The purpose of this test is to assess the accuracy of GAIA at reproducing the bed evolution in an alluvial channel bend under unsteady-flow conditions. The mechanics of sediment transport in channel bends, frequently appearing in natural rivers, are much more complex than that in straight channels. The complexity is twofold. On the one hand, the sediment transport in a channel bend is subject not only to longitudinal transport but also to transverse transport and transverse sorting by the secondary flow inherently associated with bends. On the other hand, the unsteadiness of flow in natural rivers certainly has some effects on the structure of the flow field, thereby affecting the motion of sediment particles.

This test is the experimental setup (RUN 5) proposed by Yen and Lee (1995). In this case, the bed evolution of a 180° channel bend with an initial flat bottom is computed for a triangular-shaped 300 minhydrograph. Numerical results are validated by measured contours of bed evolution after at the end of the experience and by measured bottom elevations at two different cross sections (90° and 180°). This validation case can be performed for uniform or graded sediment distribution.

### 5.2 Problem setup

The flume consists of a straight section of 11.5 m long, a 180° bend of 4.0 m radius and a downstream straight section of 11.5 m long, with a constant slope in flow direction equal to 0.002. The width of the flume channel is 1.0 m. A triangular-shaped inflow hydrograph with an initial discharge of  $Q = 0.02 \text{ m}^3/\text{s}$ , a water depth at the outflow of  $h = 0.0544 \text{ m}$  and a peak discharge of equal to  $0.053 \text{ m}^3/\text{s}$  (water depth  $h = 0.103\text{m}$ ) at  $T = 100 \text{ min}$  is used, see Figure 17.1. After  $T = 100 \text{ min}$ , the inflow discharge is reduced linearly until it reached the initial values at the end of the experiment ( $T = 300 \text{ min}$ ).

The sediment of the experiment has a median diameter of  $D_{50} = 1 \text{ mm}$ . Five sediment classes with diameters  $D = 0.31, 0.64, 1.03, 1.69$  and  $3.36 \text{ mm}$  are chosen to reproduce the sediment distribution of the experiment. An initial distribution of 20% for each class is adopted. The Engelund-Hansen formula is adopted to estimate the sediment transport capacity of the channel. The slope effect and the secondary currents correction are accounted for this test. The influence of the slope effect on the the direction of the bedload transport is accounted through the Talmon formula, with  $\beta_2 = 0.85$ . The influence of the slope effect on the the magnitude of the bedload transport is accounted through the Soulsby formula, with an friction angle of 35°. The default

value of  $\alpha = 1$  is used for the secondary currents parameter, therefore the Engelund parameter  $A = 7$ . The Continuous Vertical Sorting Model has been choosed as layer model. The total thickness of the 20 cm is maximal discretised by 100 sections. For the active layer thickness the formulation of Malcherek has been selected. Initially a uniform distribution is assumed.

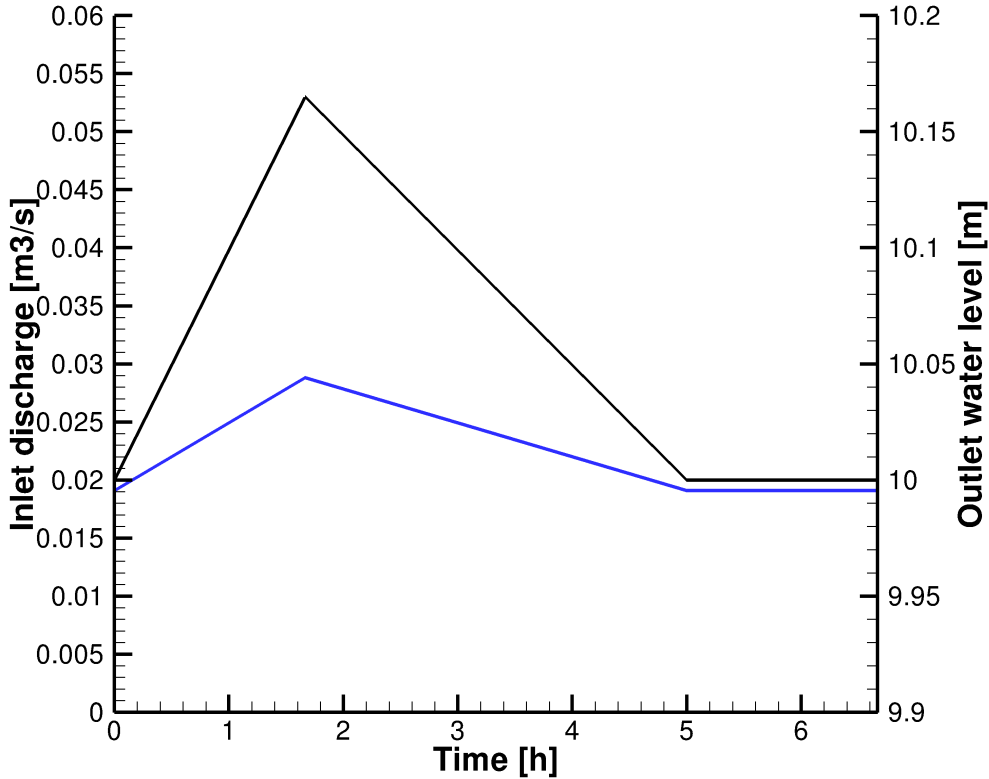


Figure 5.1: Triangular-shaped hydrograph.

A friction closure relationship, based on the Nikuradse roughness length is adopted to account for the bed resistance. For this case,  $k_s = 3.5$  mm ( $\approx 3 \times D_{50}$ ) and the Elder model is specified to parameterize the turbulent eddy viscosity. The critical Shields parameter is set at 0.047 and the bed porosity is 0.375.

### 5.3 Numerical setup

Numerical simulations were conducted on an unstructured, triangular finite element mesh with 3230 elements and 1799 nodes and a mean grid size of the order of 0.20 m (Figure 17.2). As initial condition, a fully developed (stationary) flow with a constant water-depth  $h = 0.0544$ m and discharge  $0.02\text{ m}^3/\text{s}$  is imposed and the bottom has a constant slope in flow direction equal to 0.002.

The time step is set to 0.5 s. For a mean velocity in the range  $[0.37 - 0.53]$  m/s and a mean grid size of the order of 0.2 m, the mean Courant number varies between 0.6 and 1.3.

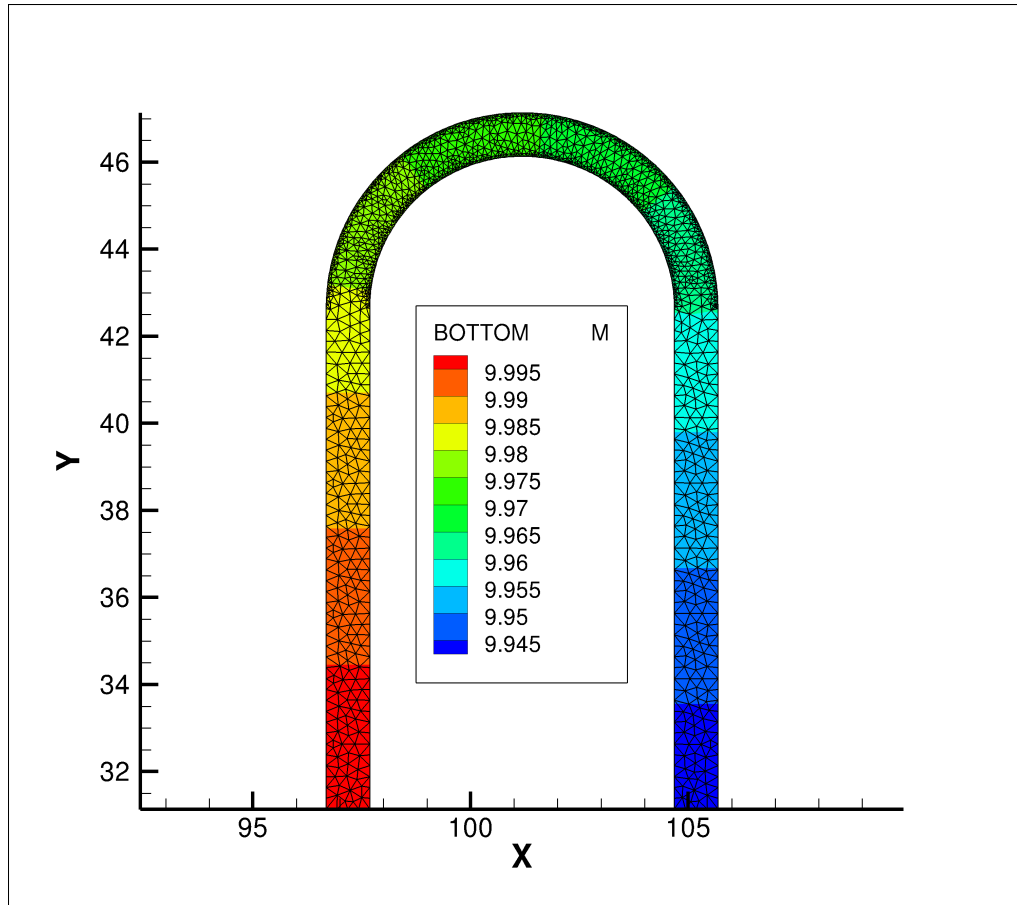


Figure 5.2: Finite element discretization of the bend.

## 5.4 Results

Numerical results of the normalized bed evolution are shown in Figure 5.3. Morphological changes exhibit the expected patterns of erosion and sedimentation at the channel bend, with the presence of a point bar along the inner-bank and a deeper channel along the outer-bank of the bend. The computed bed changes are in agreement with the measured data. Without accounting for the secondary flow effect, one cannot obtain such reasonable results. Numerical and observed bottom profiles at cross sections  $90^\circ$  and  $180^\circ$  are presented in Figure 5.4 for a total time equal to 5 hs. In Figure 5.5 the comparison of measured and simulated mean diameter for the cross section  $90^\circ$  is presented. Both simulation and measurement show the expected coarser sediment at the outer bend and the finer sediment at the inner bend.

## 5.5 References

Yen, C. and Lee, K.T. (1995) *Bed Topography and Sediment Sorting in Channel Bend with Unsteady Flow*. Journal of Hydraulic Engineering, Vol.121, No. 8.

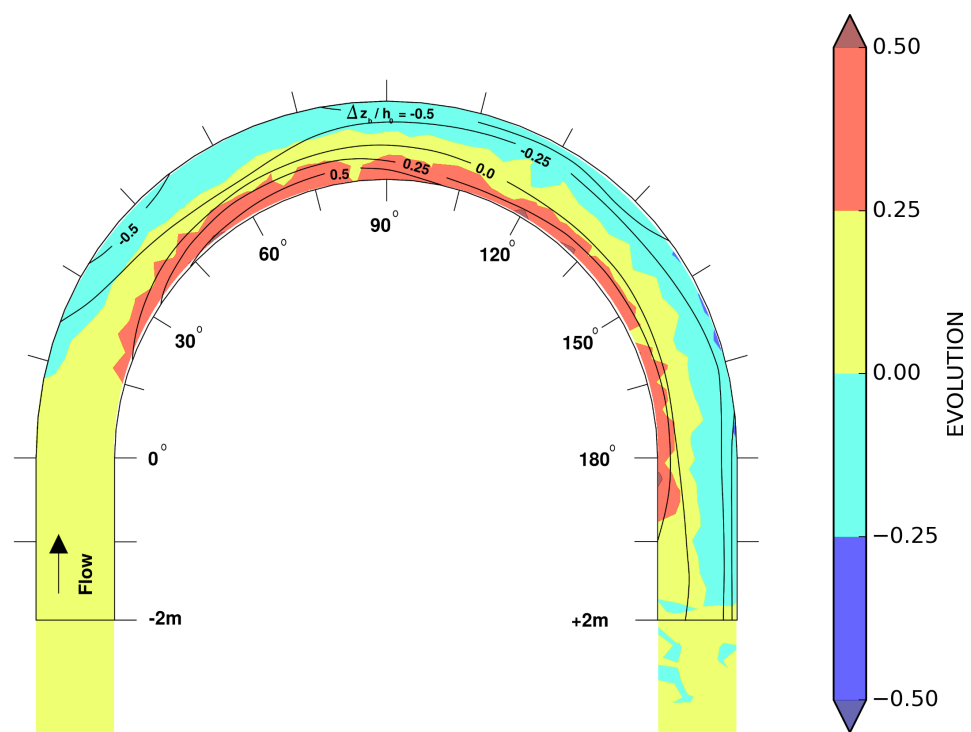


Figure 5.3: Comparison of simulated (coloured) and measured (black contour lines) normalized bed evolution.

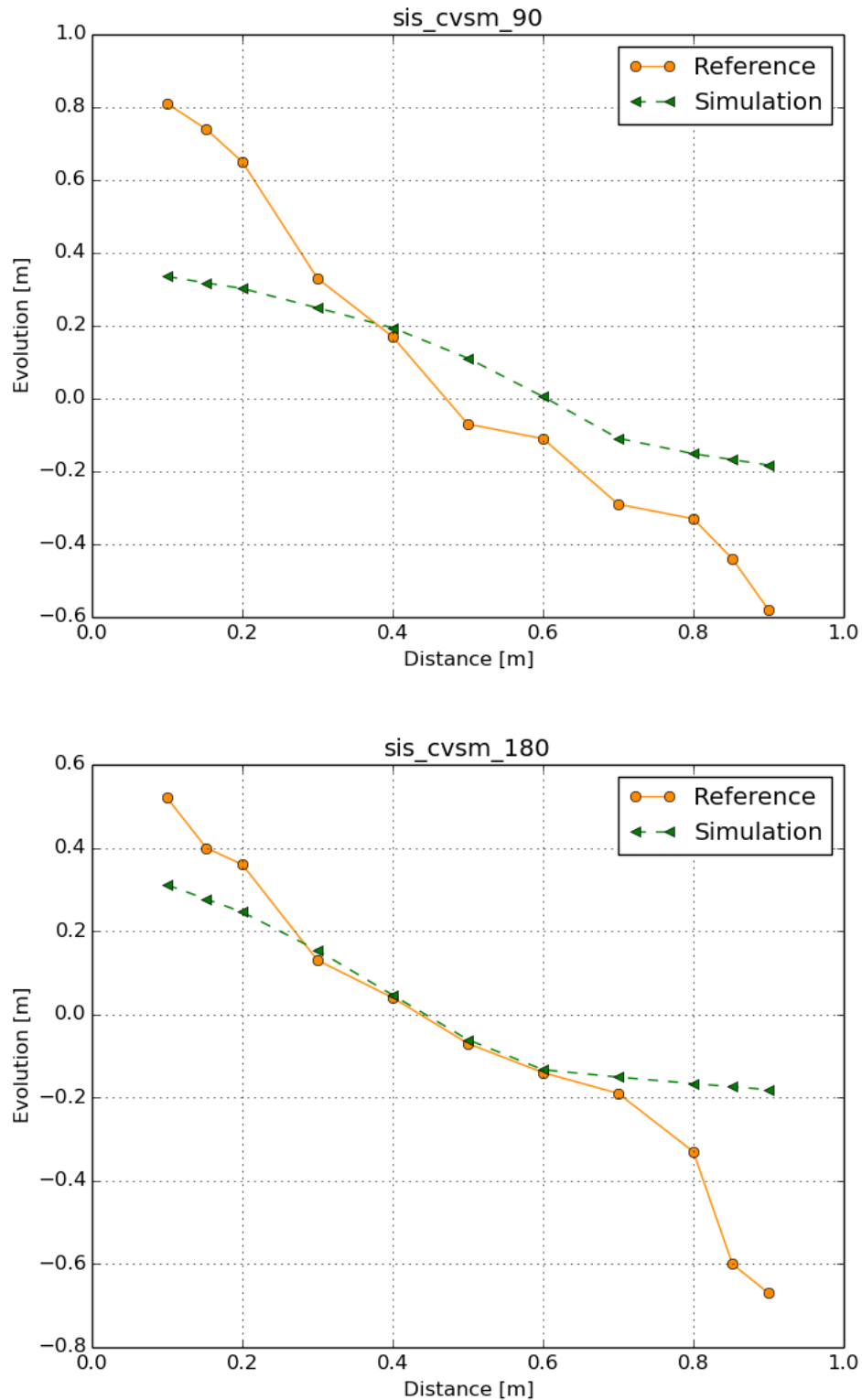


Figure 5.4: Comparison of simulated and measured bottom elevation at cross section 90° and 180°.

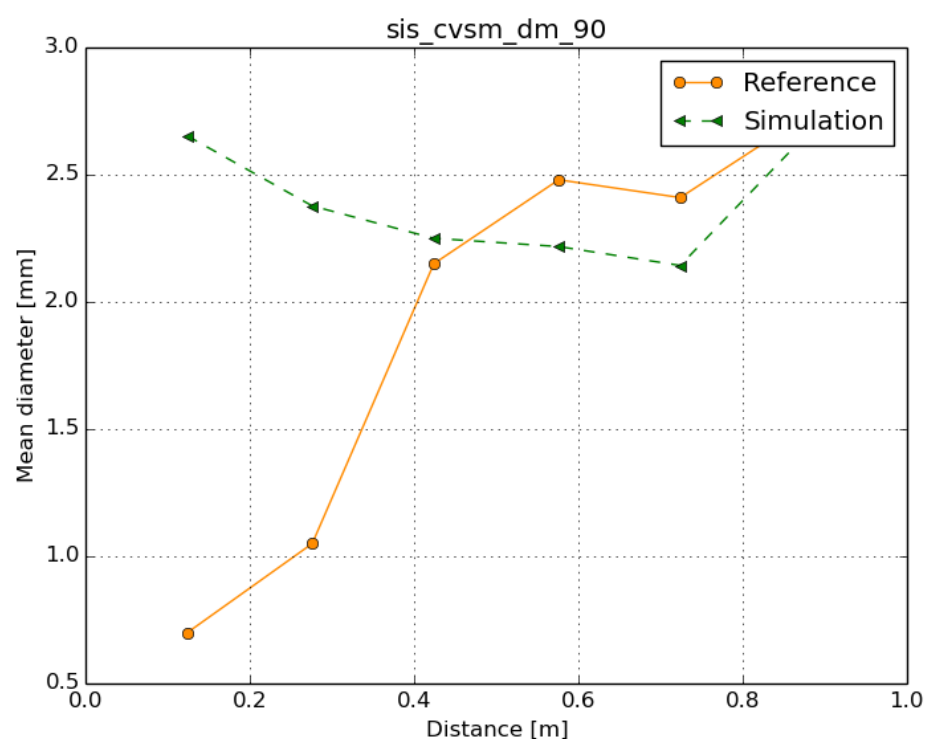


Figure 5.5: Comparison of simulated and measured mean diameter at cross section 90°

## 6. flume\_bc

### 6.1 Purpose

The aim of this test case is to verify the solid discharge imposition in a upstream open boundary.

### 6.2 Description

This test case is inspired by the laboratory experiment of [18]. This is a straight channel for which a quantity of sediment is injected at the entrance.

### 6.3 Physical parameters

The simulation duration is 30 minutes, which correspond to 1800 s. A Manning-Strickler's friction law is used on the bottom with a coefficient of  $62 \text{ m}^{1/3}/\text{s}$ . No turbulence model is used. The sediment are non-cohesive and are transported with the Meyer Peter Muller formula. The considered sediment diameter is 0.32 mm with a density of  $2650 \text{ kg/m}^3$ .  
No skin friction correction is considered.

#### 6.3.1 Geometry and Mesh

The length of the flume is 30 m and its width is 1 m. Figure 6.1 shows the mesh with a size of 0.1 m. The slope is 0.427 % and figure 6.2 shows the bottom elevation in the domain at the initial time.

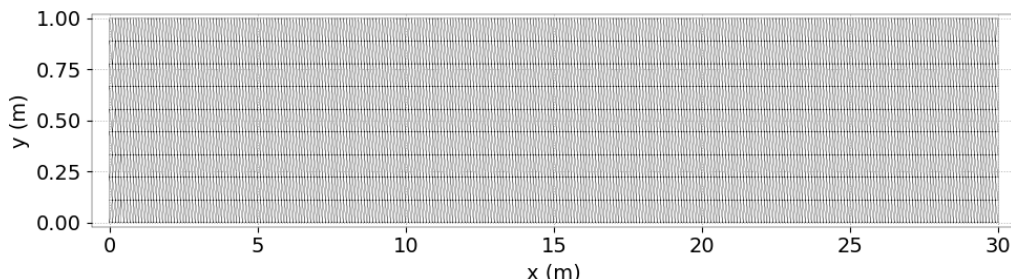


Figure 6.1: Mesh of the flume.

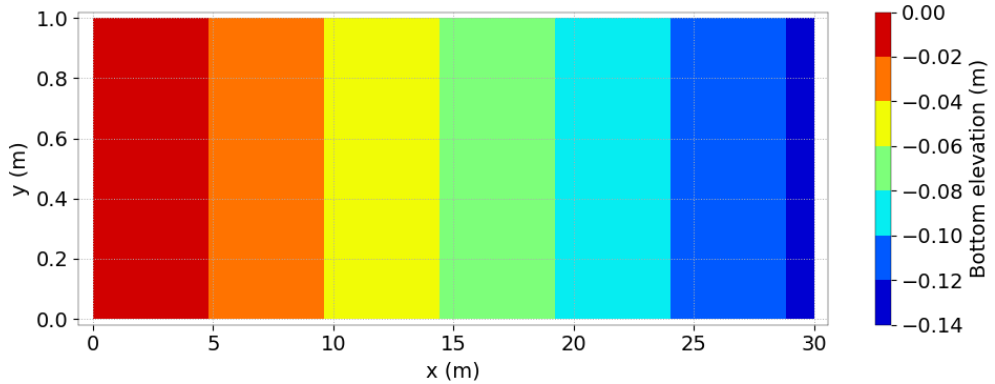


Figure 6.2: Initial bottom elevation on the flume.

## 6.4 Initial and Boundary Conditions

### 6.4.1 Initial conditions

The initial condition for the water depth is a constant depth of 0.041 m in the flume. The initial velocity is set to  $u = \frac{q}{h}$  with  $q$  the imposed discharge  $0.0355 \text{ m}^3/\text{s}$  and  $h$  the initial water depth. This results in an initial velocity of  $0.8659 \text{ m/s}$  in the x-axis orientation and  $0 \text{ m/s}$  in the y-axis orientation.

### 6.4.2 Boundary conditions

The imposed discharge at the upstream is  $0.0355 \text{ m}^3/\text{s}$  and the downstream imposed elevation is  $0.0528 \text{ m}$ . The solid discharge is imposed in the upstream boundary with a value of  $6.4528 \times 10^{-5} \text{ kg/s}$ . In case of a bedload boundary file, the value of the imposed discharge is interpolated from  $0 \text{ m}^3/\text{s}$  at the initial time to  $6.4528 \times 10^{-5} \text{ kg/s}$  at the final time. 6 scenarios are tested and the table 6.1 describes them.

Case	Solid discharge	Sediment classes	Classes initial fraction	Distribution
1	Constant	NCO	1.	Free
2	Constant	NCO,NCO	0.4,0.6	Free
3	Variable	NCO	1.	Free
4	Variable	NCO,NCO	0.4,0.6	Free
5	Constant	CO,NCO,NCO	0.2,0.3,0.5	Free
6	Constant	NCO,NCO	0.4,0.6	Imposed (0.6,0.4)

Table 6.1: Cases tested.

## 6.5 Numerical parameters

The Kinetic finite volume scheme is used to compute hydraulic variables from the shallow water equations and finite volume upwind scheme is used to solve Exner equation.

## 6.6 Results

### 6.6.1 Case 1

Figure 6.3 shows the longitudinal profile of the bottom elevation at the end of the simulation.

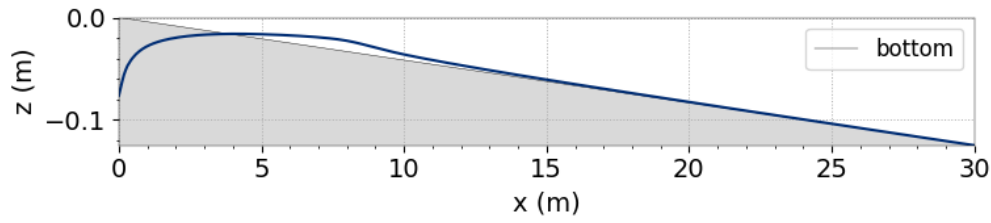


Figure 6.3: Final bottom elevation on the flume.

Figure 6.4 shows the imposed discharge during the time, extracted from the listing.

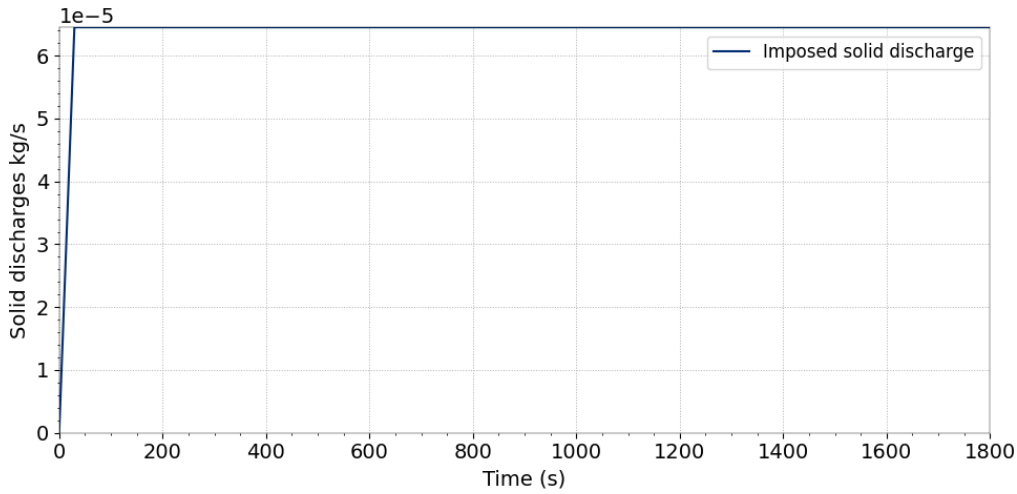


Figure 6.4: Solid discharge imposed during the simulation.

### 6.6.2 Case 2

Figure 6.5 shows the imposed solid discharge for each class during the time, extracted from the listing.

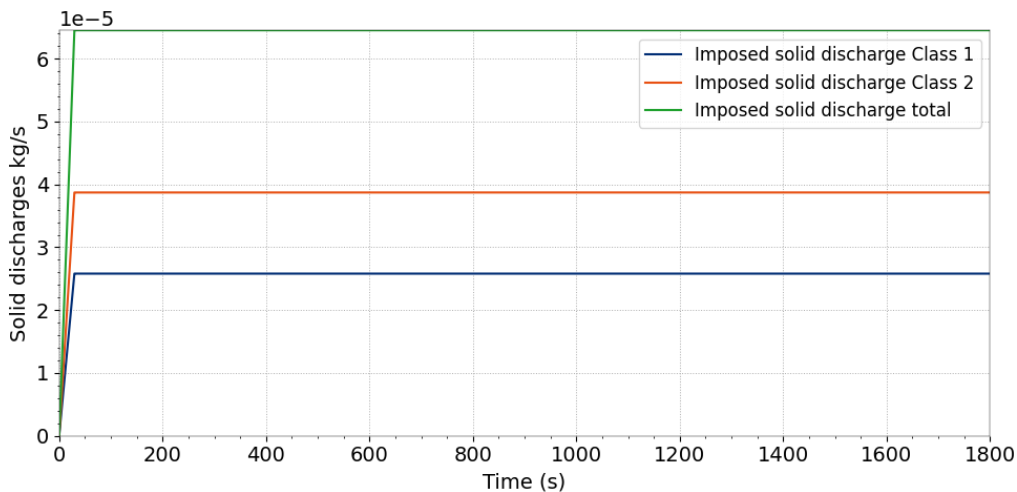


Figure 6.5: Solid discharge imposed during the simulation.

### 6.6.3 Case 3

Figure 6.6 shows the imposed solid discharge during the simulation, extracted from the listing.

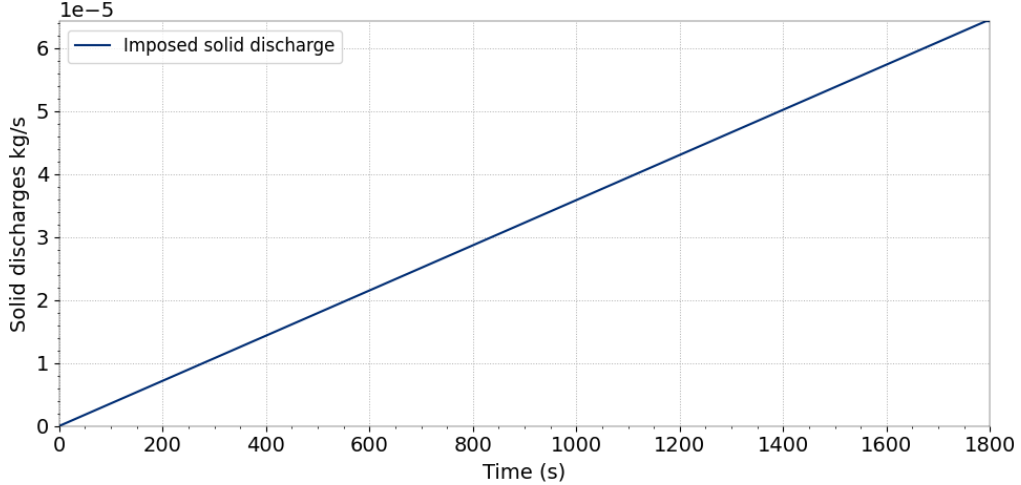


Figure 6.6: Solid discharge imposed during the simulation.

### 6.6.4 Case 4

Figure 6.7 shows the imposed solid discharge for each class during the simulation, extracted from the listing.

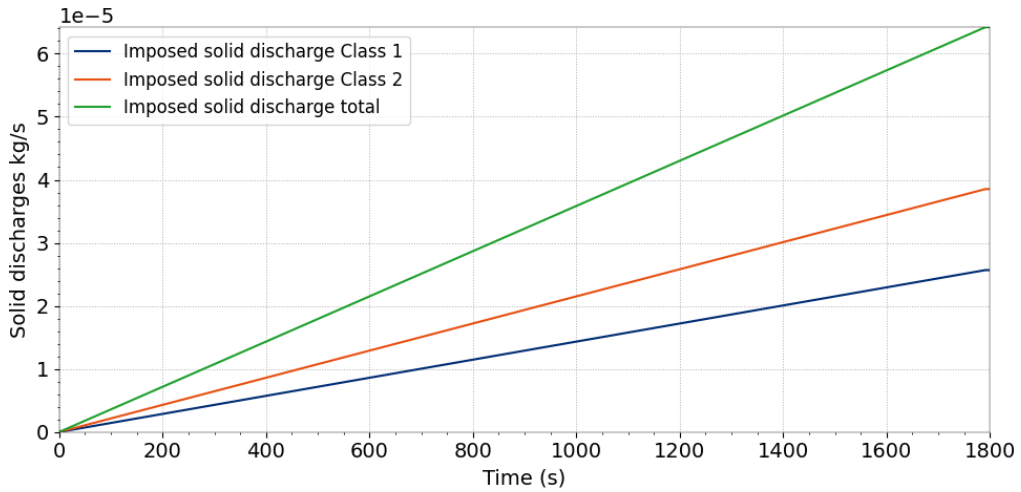


Figure 6.7: Solid discharge imposed during the simulation.

### 6.6.5 Case 5

Figure 6.8 shows the imposed solid discharge for each class during the simulation, extracted from the listing.

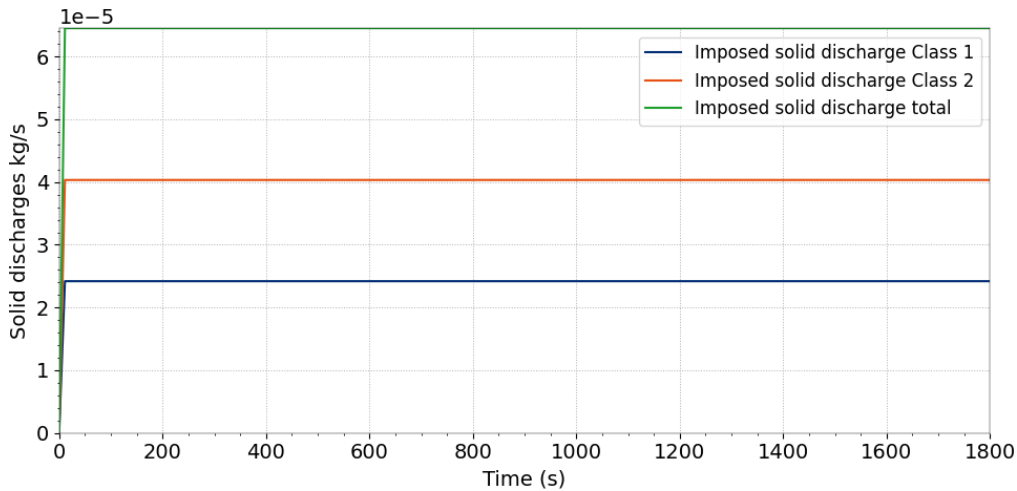


Figure 6.8: Solid discharge imposed during the simulation.

### 6.6.6 Case 6

Figure 6.9 shows the imposed solid discharge during the simulation, extracted from the listing.

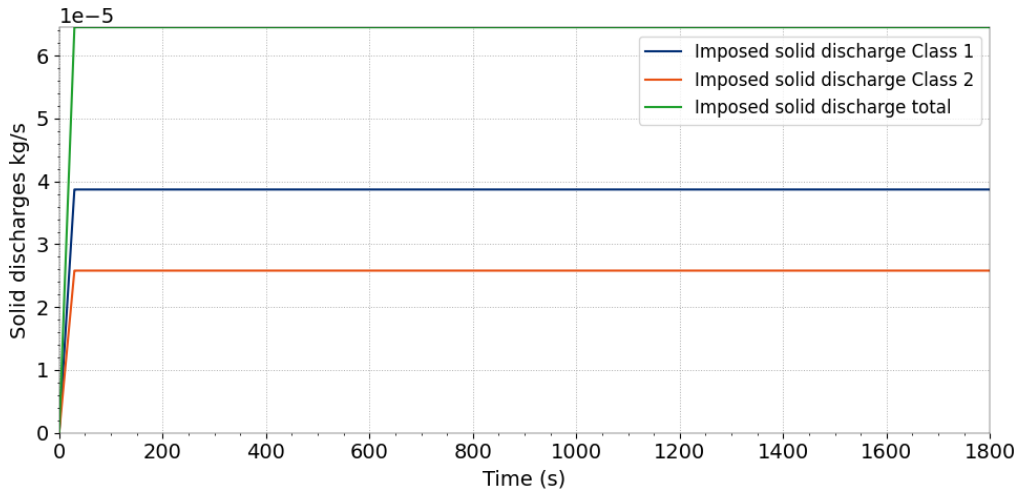


Figure 6.9: Solid discharge imposed during the simulation.

## 6.7 Conclusion

The model is able to impose a solid discharge:

- constant or variable in time;
- with several classes, even with simulation with both cohesive and non-cohesive material;
- with a prescribed sediment distribution, or a free sediment distribution.

## 7. guenter-t2d

### 7.1 Purpose

The aim of this test case is to evaluate the ability of GAIA to represent the sediment distribution in an experimental flume.

### 7.2 Description

This test case represents 2 of the 10 flume experiments done in [7]. The experiments are noted experiment 3 and 5 in the original paper. The experiments represent a straight flume with a constant slope, an imposed discharge at the upstream and an imposed water elevation downstream. The initial sediment distribution is also different between the experiment. The measured data used here are the final bed equilibrium slope, and the final sediment distribution for each experiment.

### 7.3 Physical parameters

The experiments last approximatively a month of physical time but the equilibrium is reached within 10 to 30 hours. The duration of the computation is set to 50 hours which seems to be a good compromise between computational time and physical duration. A Manning-Strickler's friction law is used on the bottom with a coefficient of  $55 \text{ m}^{1/3}/\text{s}$ . The turbulence model used is the Elder's model, and the velocity diffusivity is set to  $10^{-6}$ .

The sediment are non-cohesive and are transported with the Meyer Peter Muller formula. A hiding factor is taken into account in a user fortran and corresponds to the Parker-Klingeman formulation [14]:

$$H = \left( \frac{d_i}{d_m} \right)^{-0.8}, \quad (7.1)$$

where  $d_i$  is the sediment grain diameter and  $d_m$  the total mean diameter for the bed material in the active layer.

The sediment distribution is composed of 5 class with an equal distribution of 20% each. The mean diameter is then modified to respect the distribution given in the experiment. The table 7.1 gives the initial distribution measured and the corresponding distribution applied to the model.

Experiment 3	experiment	d[cm]	0.102	0.2	0.31	0.41	0.52	0.6
		%	35.9	56.7	68.6	86.1	92.8	100
	model	d[cm]	0.0285	0.0707	0.1798	0.3234	0.56	
		%	20	20	20	20	20	
Experiment 5	experiment	d[cm]	0.102	0.2	0.31	0.41	0.52	0.6
		%	57.6	78	87.5	92.7	98.3	100
	model	d[cm]	0.0354	0.0708	0.1135	0.2232	0.5534	
		%	20	20	20	20	20	

Table 7.1: Initial sediment distribution.

### 7.3.1 Geometry and Mesh

Figure 7.1 shows the initial bottom elevation and the mesh for the two experiments. The initial slope of experiment 3 is 0.25% and of experiment 5 is 0.35%.

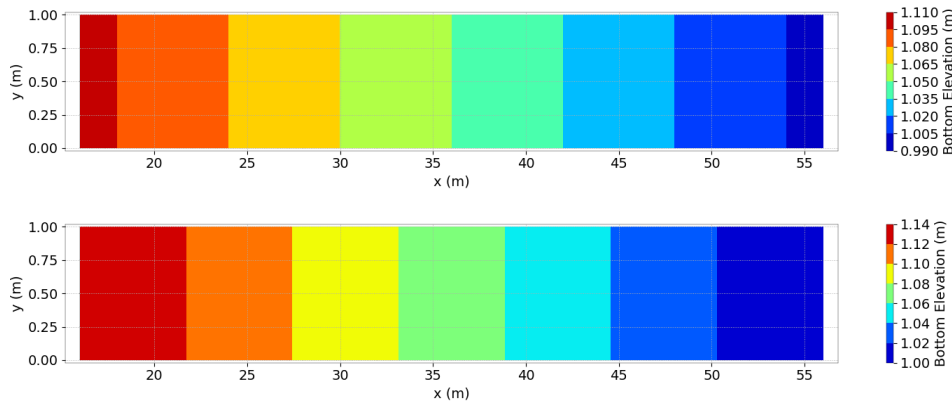


Figure 7.1: Bottom elevation and mesh for exp 3 (top) and exp 5 (bottom).

## 7.4 Initial and Boundary Conditions

### 7.4.1 Initial conditions

The initial condition is set with a previous computation file. This file is generated for a hydraulic computation only, with a computational time which allows to reach a steady state.

### 7.4.2 Boundary conditions

For the experiment 3, the imposed discharge at the upstream is  $0.056 \text{ m}^3/\text{s}$  and the downstream imposed elevation is 1.098 m, knowing that the initial bottom elevation is 1 m.

For the experiment 5, the imposed discharge at the upstream is  $0.031 \text{ m}^3/\text{s}$  and the downstream imposed elevation is 1.0653 m, knowing that the initial bottom elevation is 1 m.

## 7.5 Numerical parameters

The SUPG finite element scheme is used to compute hydraulic variables from the shallow water equations and a finite volume centred scheme is used to solve the Exner equation.

## 7.6 Results

Figure 7.2 shows the bottom evolution at the end of the simulation.

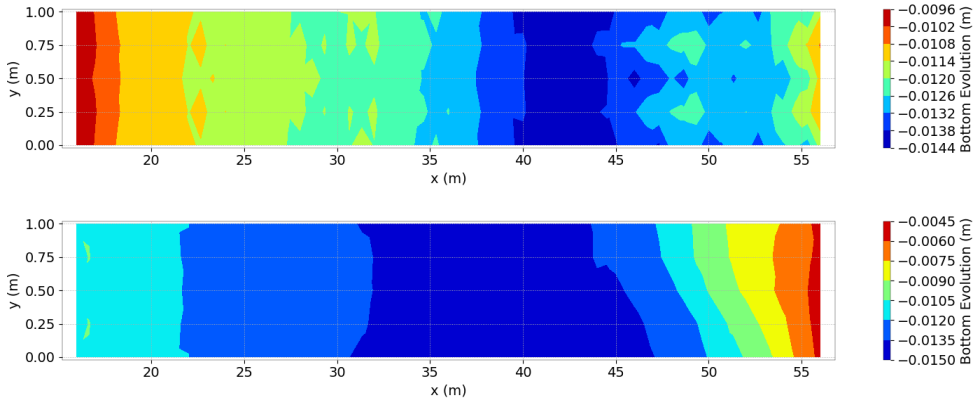


Figure 7.2: Bottom evolution for exp 3 (top) and exp 5 (bottom).

Figure 7.3 shows the bottom elevation at the end of the simulation.

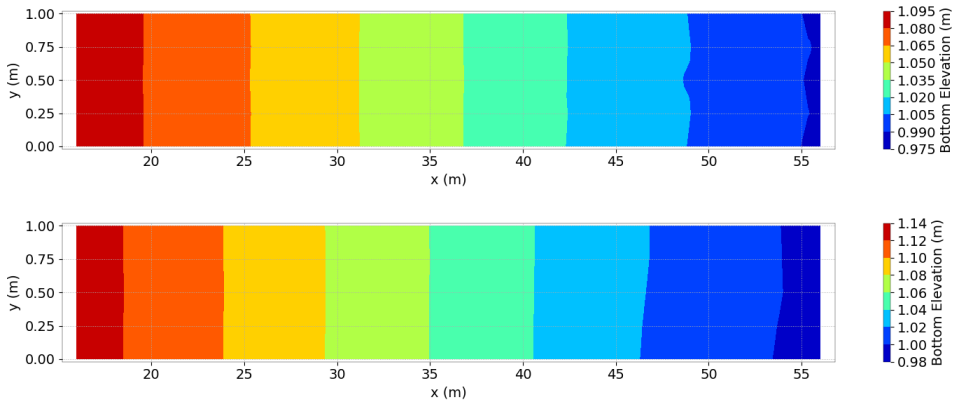


Figure 7.3: Final bottom elevation for exp 3 (top) and exp 5 (bottom).

Figure 7.4 shows a longitudinal profile of the initial bed elevation, final bed elevation compared to experimental equilibrium slope.

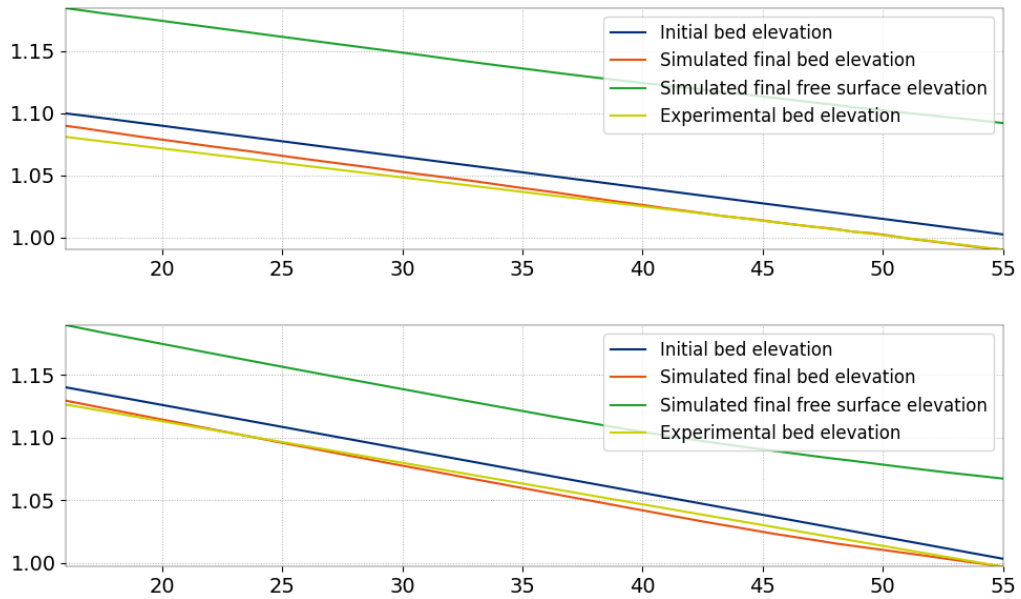


Figure 7.4: Final bottom elevation for exp 3 (top) and exp 5 (bottom) compared to the experimental equilibrium slope.

Figure 7.5 shows the initial distribution and the final distribution compared to the measured one.

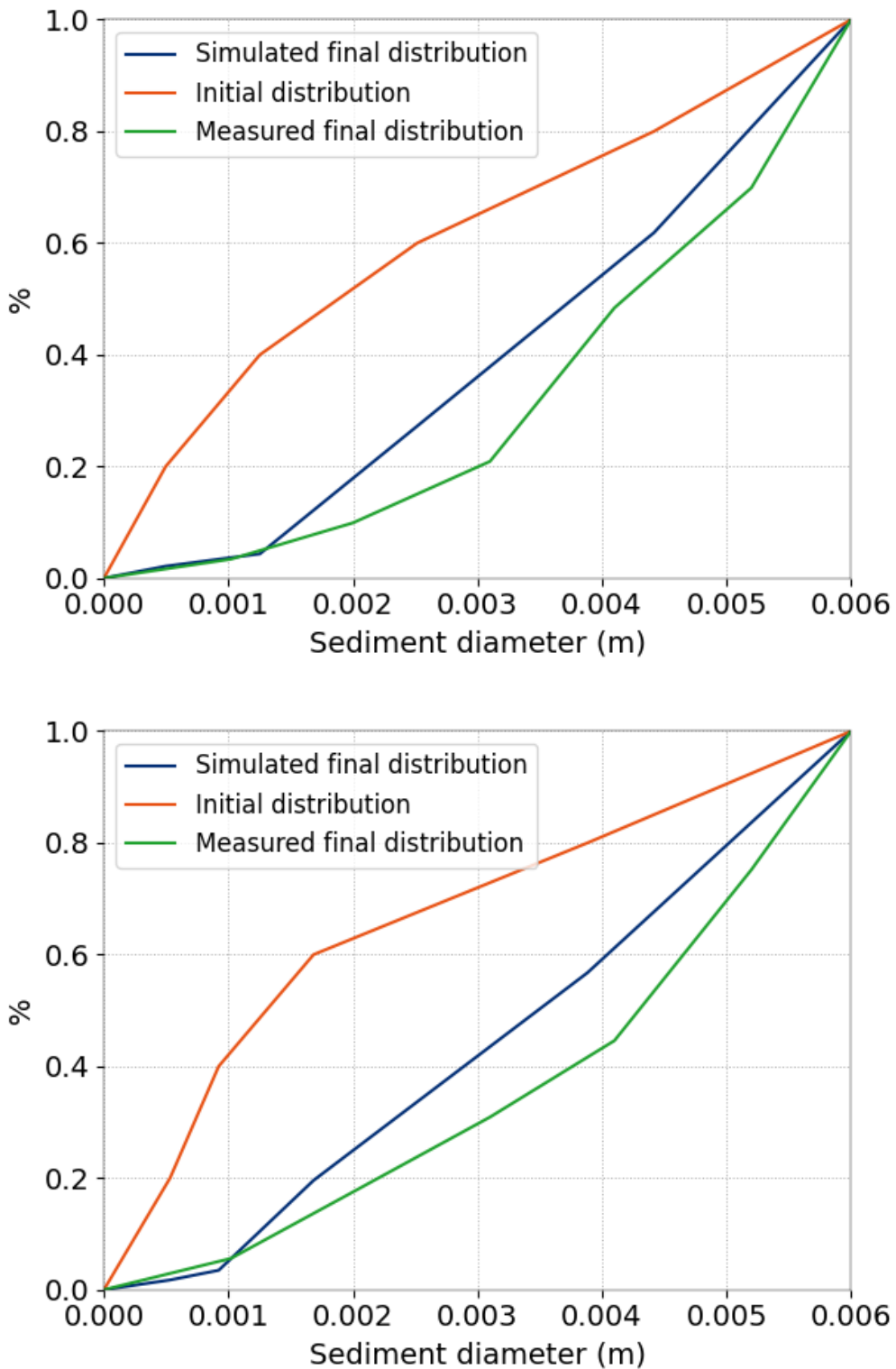


Figure 7.5: Sediment distribution for exp 3 (top) and exp 5 (bottom).

## 7.7 Conclusion

The model is able to reproduce correctly both the erosion slope and the sediment distribution at the end of the simulation, and those while the calibration parameters are the same for both experiment.

## 8. hippodrome-t2d

### 8.1 Purpose

A racetrack shape configuration has been adopted during the earlier developments of GAIA to assess its conservativeness properties, to test its ability at reproducing bed and layer thicknesses evolutions and to optimize the code implementation within the new module structure. The same configuration has been chosen to test different sediment transport processes in 2D, namely:

- t2d\_1C0s: suspended sediment transport, cohesive sediment, 1 sediment class.
- t2d\_1NC0b: bedload transport, non-cohesive sediment, 1 sediment class.
- t2d\_1NC0b\_vf: idem previous case, finite volume.
- t2d\_1NC0s: suspended sediment transport, non-cohesive sediment, 1 sediment class.
- t2d\_4NC0b: bedload transport, non-cohesive sediment, 4 sediment classes.
- t2d\_4NC0b\_vf: idem previous case, finite volume.
- t2d\_4NC0b\_strat\_vf: bedload transport, non-cohesive sediment, 4 sediment classes, stratigraphy discretization with 3 layers.

To simplify the involved physical processes, the wind is considered as the only driving force of the flow. This test case can be useful to users who want to test their own developments on a simple configuration. The documentation presented here only refers to the case t2d\_1NC0b.

### 8.2 Description

#### 8.2.1 Geometry, initial bathymetry and mesh discretization

The computational domain and finite element discretization are showed in Figure 8.1.

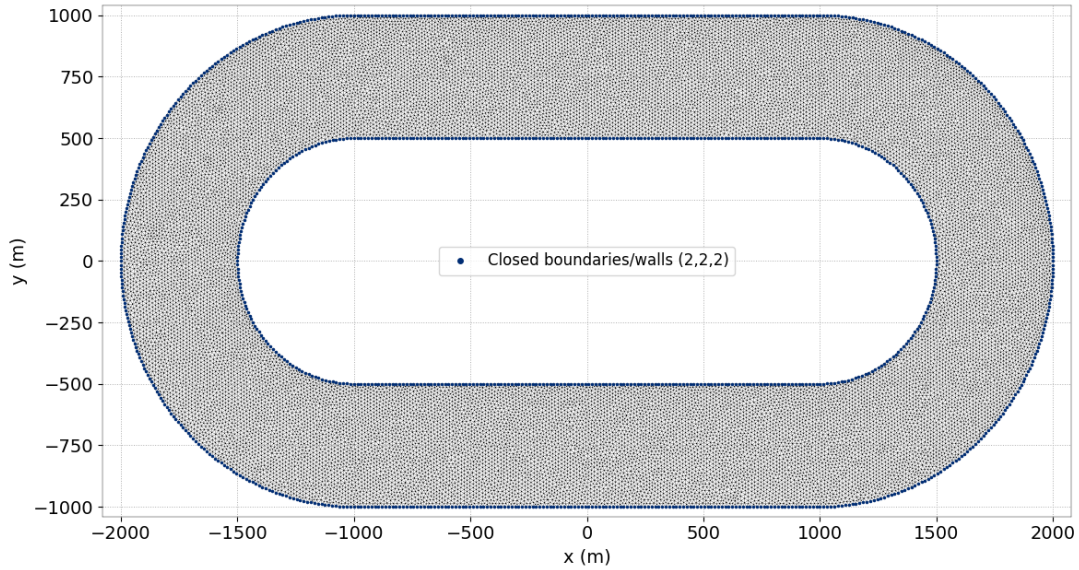


Figure 8.1: Mesh discretization of the *hippodrome-t2d* test case.

### 8.2.2 Bathymetry

The bump and the lateral banks in the initial bathymetry favor the bed evolution on both longitudinal and lateral slopes, see Figure 8.2. Lateral banks allow the formation of dry areas in the computational domain.

### 8.2.3 Initial conditions

A fluid-at-rest is imposed as initial condition with constant elevation equal to 5m and zero velocity field.

### 8.2.4 Boundary conditions

No liquid boundaries are included in the numerical simulations. Only wall-type conditions are imposed at the internal and external domain boundaries, see Figure 8.1.

### 8.2.5 Physical and numerical parameters

This test case accounts for bedload transport of uniform, non-cohesive sediment of diameter 0.0002m. Sediment fluxes are computed with the Soulsby-van Rijn total sediment transport capacity formula.

## 8.3 Results

Figure 8.2 shows the evolution of the bottom from time 0s to 10000s for case t2d\_1NC0b. As expected, scouring processes next to the bump as well as sediment accretion inside the trench are observed.

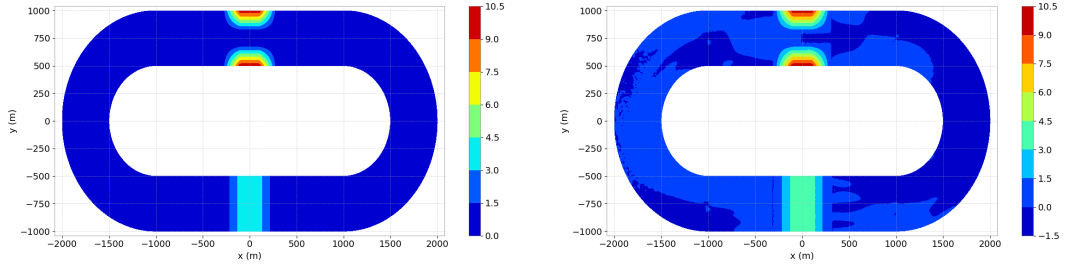


Figure 8.2: Bed evolution at times 0s and 10000s.

#### 8.4 Conclusion

This test provides a starting point to set-up 2D morphodynamic applications as well as a simplified configuration for quick code *debugging* and testing.

## 9. Littoral

### 9.1 Purpose

This test case illustrates the setup of a three-way coupling problem waves, currents and sediment transport.

### 9.2 Description of the problem

A wave, current and sediment transport simulation in a straight, uniform stretch of coastline is considered. The beach is located at  $y = 200$  m, the sloping bed is imposed in subroutine `corfon`. The offshore depth is 10 m. This is the classical test case of a rectilinear beach with sloping bed. The model allows to calculate the littoral transport. ! This test case illustrates the effect of waves which is :

- to generate the current induced littoral current parallel to the beach
- to increase the sand transport rate using the Bijker sand transport formula.

### 9.3 Physical parameters

#### 9.3.1 Geometry and Mesh

A domain of  $200 \times 1000$  m<sup>2</sup> is considered, with a regular mesh with elements size of the order  $\Delta x = 20$  m and  $\Delta y = 5$  m. The beach is 1000 m long, 200 m wide. The beach slope ( $Y=200$ m) is 5% and defined in `corfon.f`. The water depth along the open boundary ( $Y=0$ ) is  $h=10$ m. We use a triangular regular grid

### 9.4 Initial and Boundary Conditions

#### 9.4.1 Wave conditions

Incoming waves (waves height, period and directions) are imposed offshore at  $y = 0$ , such that  $H_s = 1$  m,  $T_p = 8$  s. The Jonswap spectrum is used. The waves direction is 30 deg relative to the  $y$ -axis. The mesh is as shown on Figure 9.1

### 9.5 Numerical parameters

⇒ Offshore ( $Y=0$ ): Offshore wave imposed/no littoral current/no set up

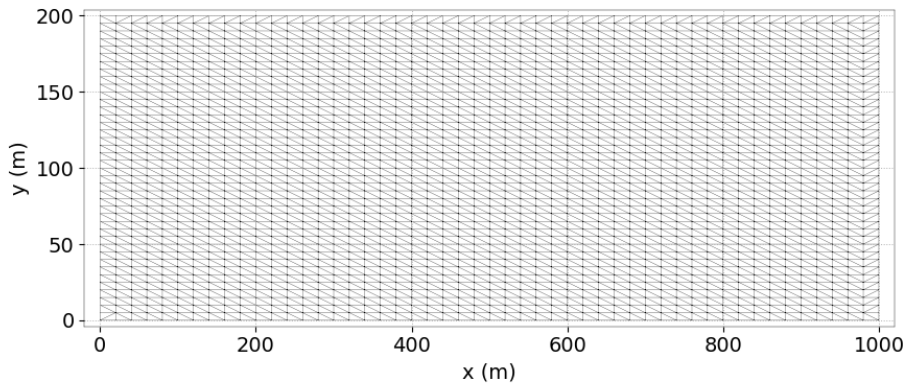


Figure 9.1: mesh of the case littoral

Tomawac: The wave height is imposed on the offshore boundary (5 4 4) ( $H_s=1\text{m}$ ), for a wave period ( $T_p=8\text{s}$ ).

Telemac2D: The current and free surface are imposed to 0 along the offshore boundary (5 5 5).

## 9.6 Results

Results (littoral current and transport rates) as well as wave set up/set down are in good agreement with expectations from theoretical classical results (Longuet Higgins). The model is able to reproduce the wave induced current, as well as the effect of set down/set up as the waves dissipate in the breaking zone. The sediment transport rate is located in the near shore breaking zone, where the longshore current is generated. Similar results for the littoral transport could be obtained by using an integrated formula (e.g. CERC formula).

The results are presented Figures 9.2 (Velocity U) 9.3(Wave height  $H_m0$ ) and 9.4 (Bed Shear stress)

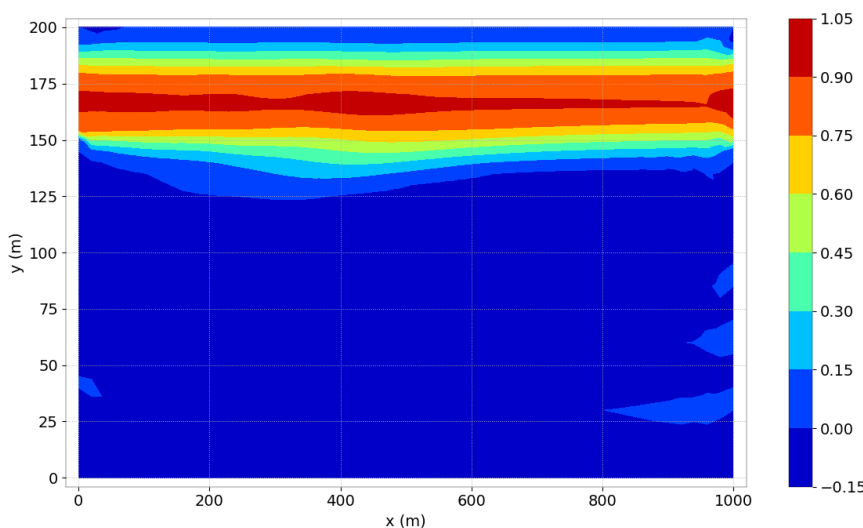


Figure 9.2: Velocity along U of the case littoral

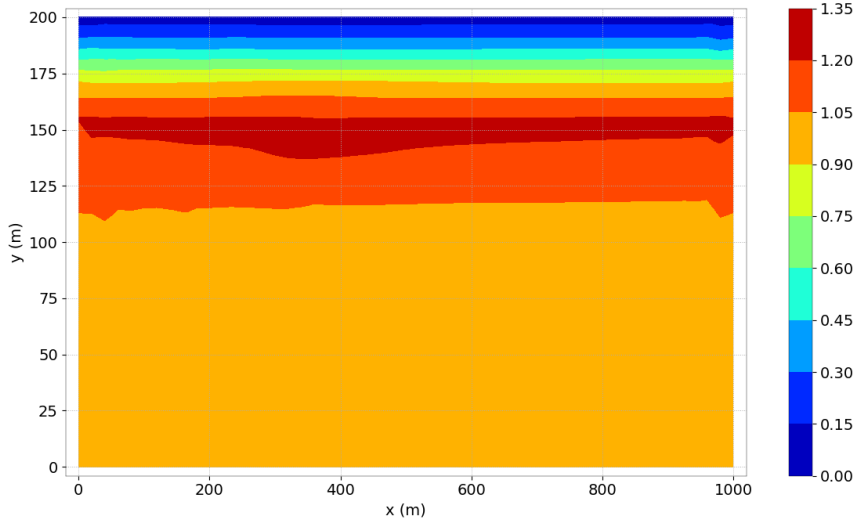
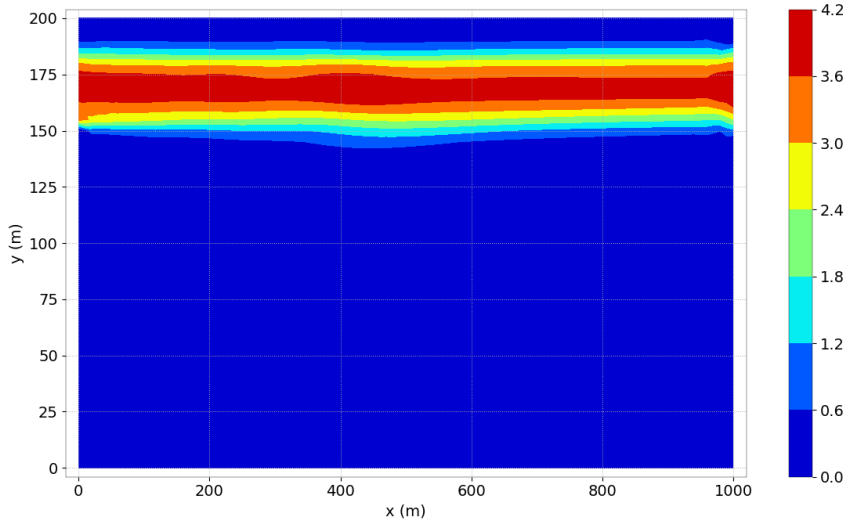
Figure 9.3: Wave heighth  $Hm0$  of the case littoral

Figure 9.4: Bed shear Stress of the case littoral

## 9.7 A new way to couple telemac2d and tomawac

On the same domain we test a new way to couple telemac2d and tomawac with different meshes, this module is called tel2tom [2]. It requires to calculate weights of interpolation before, those weights are part of the mesh. This is done using

`run_telfile.py tel2tom t2dmesh tommesh -t2d-bnd Telemac Boundary File -tom-bnd Tomawac Boundary File.`

The user will find a notebook on this use in `$HOMETEL/notebooks/pretel/tel2tom.ipynb`. In practice, in the VNV processus instead of using `run_telfile.py`, the function `connect_tel2tom` is called in the python.

In a first time we are using tel2tom using the same mesh, and in a second time using different meshes.

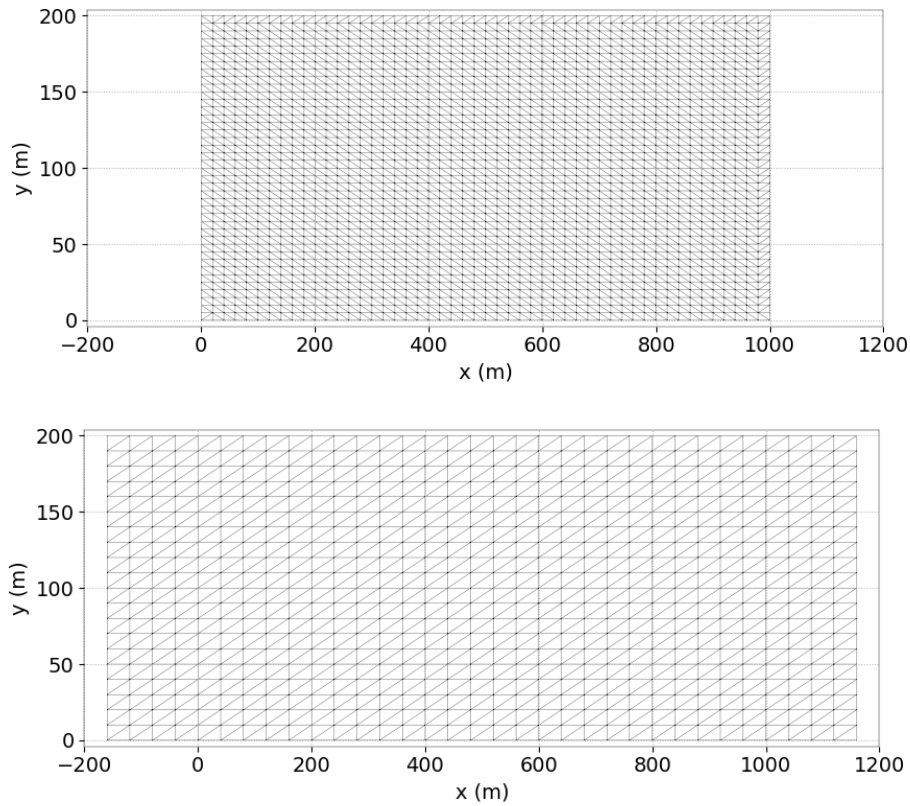


Figure 9.5: mesh of telemac2d (top) and tomawac (bottom)

### 9.7.1 Results using the same mesh

We can see that the results of Figure 9.6 9.7 and 9.8 are the same of the ones of, respectively, 9.2 9.3 and 9.4. Seeing the figures does not show that results are exactly the same, but very close. But if we use the python scripts to compute the differences between both results, we see that difference is 0.

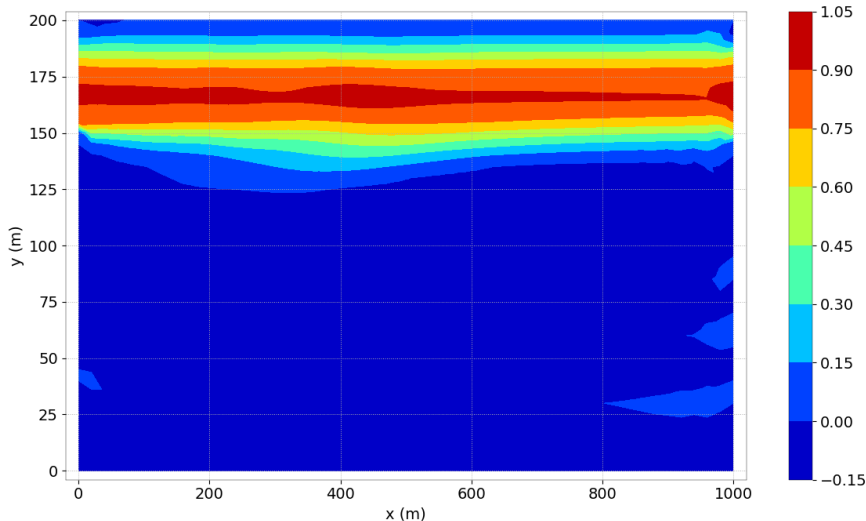


Figure 9.6: Velocity along U of the case littoral using tel2tom with the same mesh

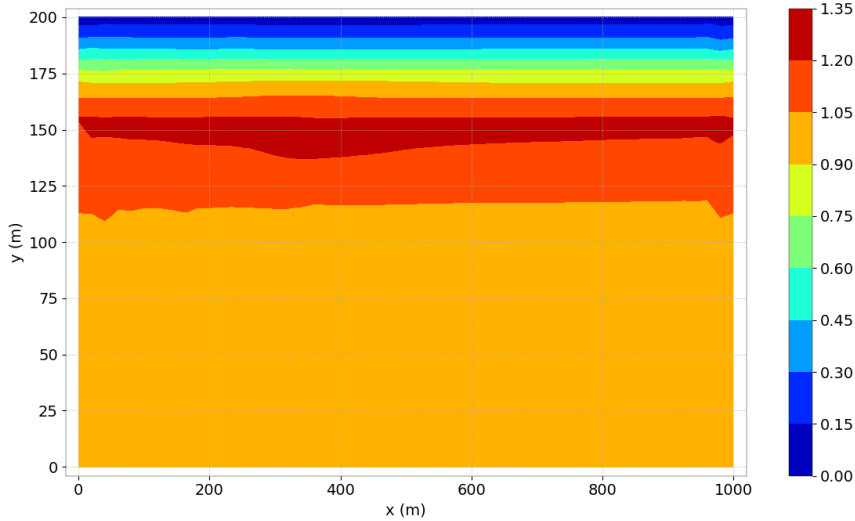


Figure 9.7: Wave heighth  $Hm0$  of the case littoral using tel2tom with the same mesh

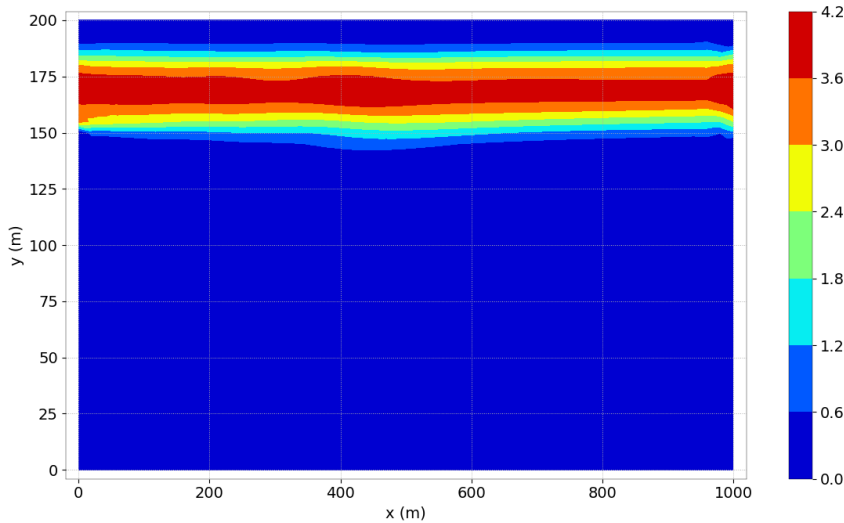


Figure 9.8: Bed shear Stress of the case littoral using tel2tom with the same mesh

### 9.7.2 Results using different meshes

We can see that the results of Figure 9.9 9.10 and 9.11 are closed to the ones of, respectively, 9.6 9.7 and 9.8.

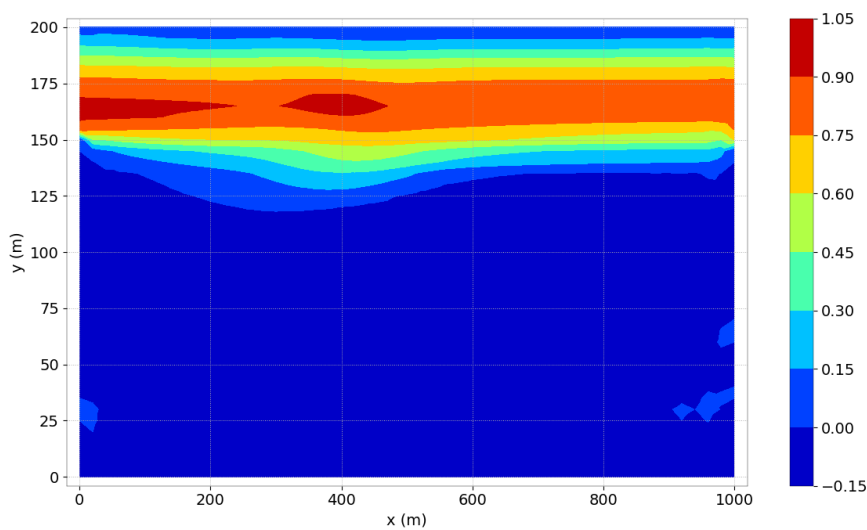


Figure 9.9: Velocity along U of the case littoral using tel2tom with different mesh

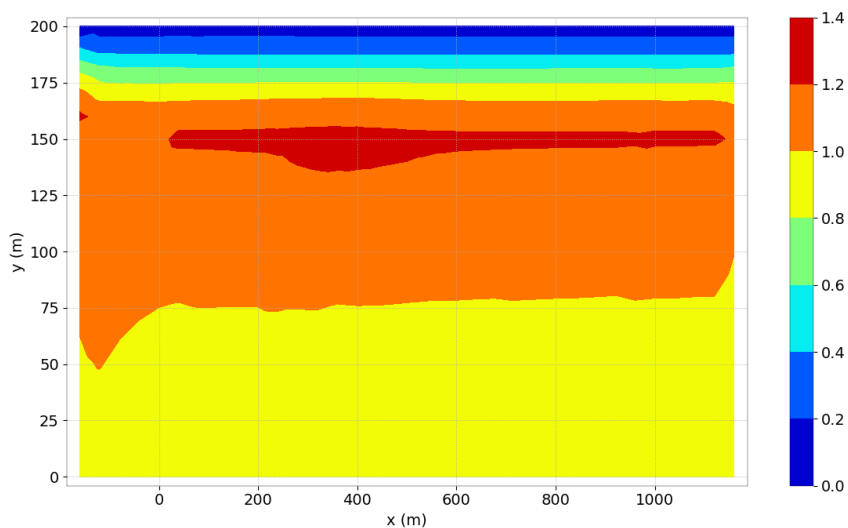


Figure 9.10: Wave height Hm0 of the case littoral using tel2tom with different mesh

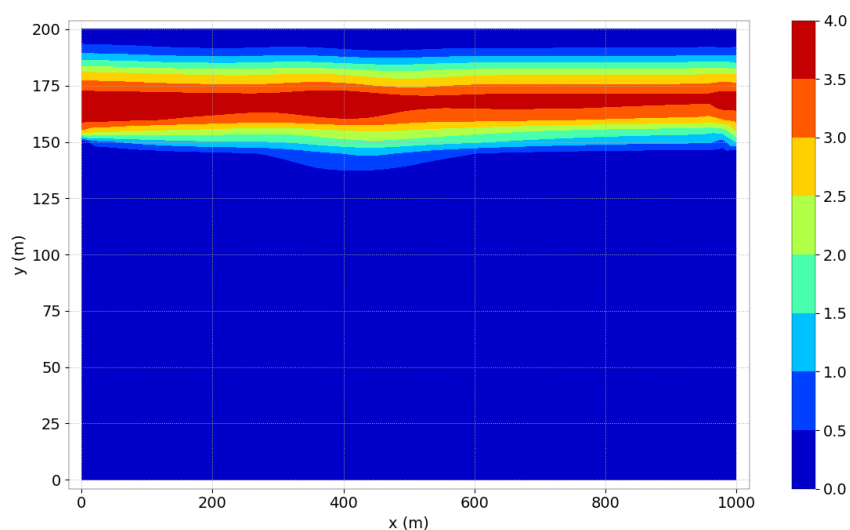


Figure 9.11: Bed shear Stress of the case littoral using tel2tom with different mesh

## **10. lyn-t3d**

Investigation is needed as this test case does not give satisfactory results with the actual steering files.

## 11. Conservation (mud\_conservation-t2d)

### 11.1 Purpose

The aim of this test is to check the mass conservation of suspended sediments for unsteady flow conditions, as well as bed mass conservation. The phenomena consists in a spreading circular wave in which a suspended sediment is released.

### 11.2 Description

#### 11.2.1 Geometry and Mesh

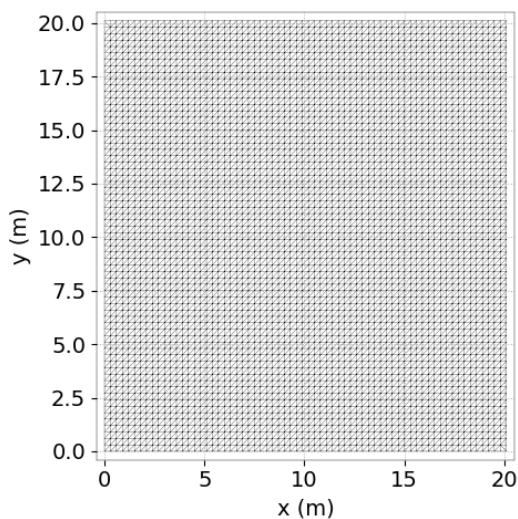


Figure 11.1: Mesh

The domain is square with a size of 20.1 m x 20.1 m with a flat bottom. The domain is meshed with 8978 triangular elements and 4624 nodes. Triangles are obtained by dividing rectangular elements on their diagonals. The mean size of obtained triangles is about 0.3 m (see figure 11.1).

### 11.2.2 Initial conditions

The fluid is initially at rest with a Gaussian free surface in the centre of a square domain (see Figure 11.2, cf. gouetteudo test case of TELEMAC-2D). Water depth is given by  $H = 2.4 \left( 1.0 + \exp \left( \frac{-(x-10)^2 + (y-10)^2}{4} \right) \right)$

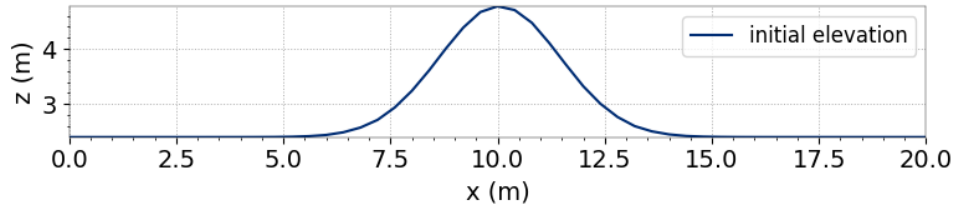


Figure 11.2: Mud conservation: initial elevation

The suspended sediment is equal to 0 everywhere except in a central zone of the domain (where the Gaussian free surface is defined) where it is equal to 1:  $C = 1$  if  $(x - 10.05)^2 + (y - 10.05)^2 < 4^2$

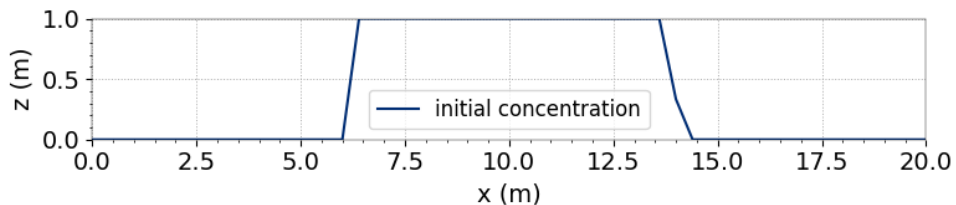


Figure 11.3: Mud conservation: initial sediment concentration

### 11.2.3 Boundary conditions

Boundaries are solid walls with perfect slip conditions.

### 11.2.4 Physical parameters

The physical parameters for hydrodynamics used for this case are the following:

- Friction: Strickler formula with  $k_s = 40 \text{ m}^{1/3}/\text{s}$
- Turbulence: Constant viscosity equal to zero (no diffusion of velocities)

The sediment is cohesive with a constant diameter equal to 0.06 mm and density equal to 1600 kg/m<sup>3</sup>. The settling velocity is set to 0.01 m/s and the Partheniades constant is set to 0.001 kg/m<sup>2</sup>/s.

### 11.2.5 Numerical parameters

## 11.3 Results

The following figures show time evolutions of the bed lost mass and the relative error of the bed layer: errors are very small.

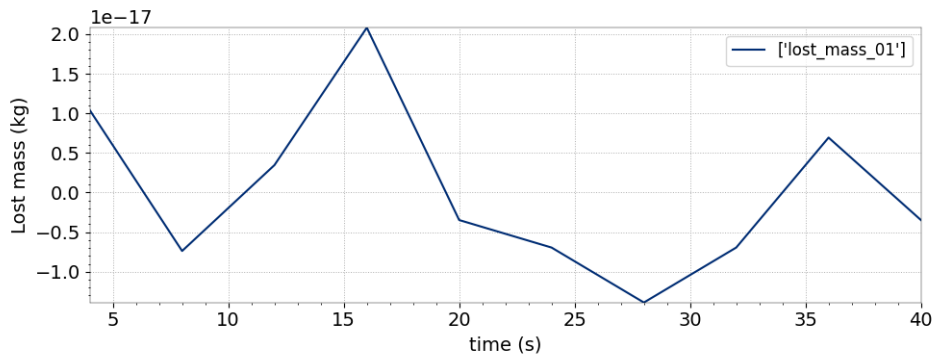


Figure 11.4: Lost mass evolution

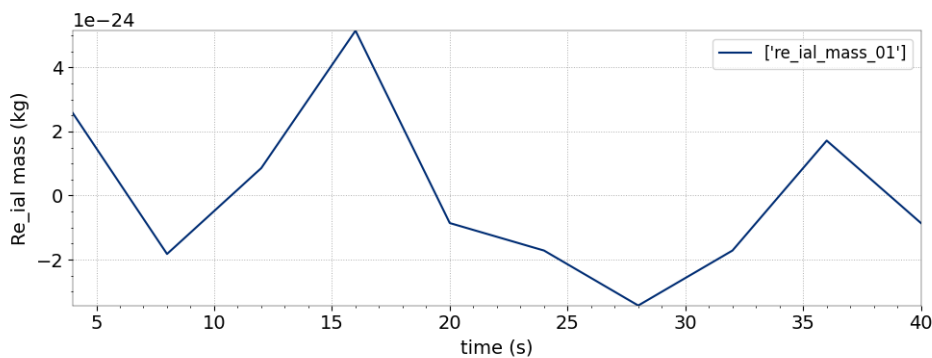


Figure 11.5: Relative mass error of bed layer

## 11.4 Conclusion

This test shows that mass is conserved for suspended sediment and bed. It is a very simple configuration which allows to quick code debugging and testing (cf. GAIA steering file where there are other commented configurations).

## 12. rouse-t3d

### 12.1 Purpose

This test validates the modeling of the hydrodynamics and non-cohesive (i.e. constant settling velocity with no turbulence damping effects) suspended sediment transport, in a permanent and uniform flow. We compare the mean flow velocities to the logarithmic profile and the sediment concentration to an analytical solution derived from the Rouse profile [1], as:

$$\frac{C_z}{C_a} = \left( \frac{(h-z)a}{(h-a)z} \right)^{\frac{w_s}{\kappa u_*}} \quad (12.1)$$

where:

$C_z$  = suspended sediment concentration at height  $z$  above the bed ( $\text{kg/m}^3$ )

$C_a$  = suspended concentration at reference height  $a$  ( $\text{kg/m}^3$ )

$h$  = water depth (m)

$w_s$  = settling velocity of the suspended sediment (m/s)

$\kappa$  = von Karman constant (= 0.41)

$u_*$  = shear velocity at the bed m/s

### 12.2 Description

The test case consists of a steady and uniform flow in a rectangular channel ( $5 \text{ km} \times 0.5 \text{ km}$ ) with flat bed, without friction on the lateral boundaries, and with friction on the bottom. The turbulence model is chosen to be consistent with the logarithmic velocity profile on the vertical (i.e. mixing length model). At the entrance of the channel, sediment is introduced with a constant concentration along the vertical, and an equilibrium profile gradually appears downstream due to combined settling and vertical diffusion.

#### 12.2.1 Geometry and Mesh

##### Bathymetry

The bathymetry consists of a flat bed with a level of -10m below mean sea level.

##### Geometry

The geometry is a rectangular channel with a length of 5 km and width of 0.5 km.

**Mesh**

The finite element mesh comprises 756 triangular elements and 444 nodes. The vertical discretisation of the model consists of 21 regularly spaced sigma planes.

### 12.2.2 Physical parameters

**Friction**

Bed friction is specified using a Nikuradse roughness length of 0.01 m

**Turbulence**

For this test case, turbulent diffusivity is most important in the vertical direction since it controls the vertical profile of the suspended concentration (along with settling velocity). Therefore, the vertical turbulence is modelled using the mixing length model of Nezu and Nakagawa. Horizontal turbulence, which is less important for this test case, is applied using a constant viscosity of 0.5 m<sup>2</sup>/s.

**Sediment**

A constant settling velocity of 0.001 m/s is used for the sediment. Flocculation is not included since this would modify the vertical profile of suspended concentration from the theoretical Rouse profile.

### 12.2.3 Initial and Boundary Conditions

**Initial conditions**

Initial conditions are set using a constant elevation of 0 m (i.e. 10 m depth) and velocities are not initialised (i.e. they start at zero). Sediment concentration is initialised to 0.1 g/L everywhere.

**Boundary conditions**

The upstream and downstream liquid boundaries are prescribed with boundary conditions to generate steady state flow with a depth average velocity of 1 m/s follows.

Upstream boundary:

- prescribed flow rate of 5,000 m<sup>3</sup>/s
- no velocity profile initialised (it forms downstream)
- prescribed constant sediment concentration of 0.1 g/L
- no concentration profile initialised (it forms downstream)

Downstream boundary:

- prescribed free surface at  $z = -0.05$  m
- free boundary for velocity

Bottom:

- solid boundary with Nikuradse bed roughness of  $k_s = 0.01$  m

Lateral wall:

- no friction

### 12.2.4 General parameters

The model was run with a time step of 30 s for a total simulation duration of 43,200 s (12 hours)

### 12.2.5 Numerical parameters

Advection for velocities and sediment: Scheme 13 (MURD3D\_POS)

### 12.2.6 Comments

## 12.3 Results

Figure 12.1 compares the theoretical [1] (i.e. logarithmic) velocity profile with the computed result and shows excellent agreement. One can see that the point at the first plane above the bottom coincides with the theoretical value, which guarantees that the friction velocity is correct.

Figure 12.2 compares the theoretical Rouse profile and the numerical solution, showing close

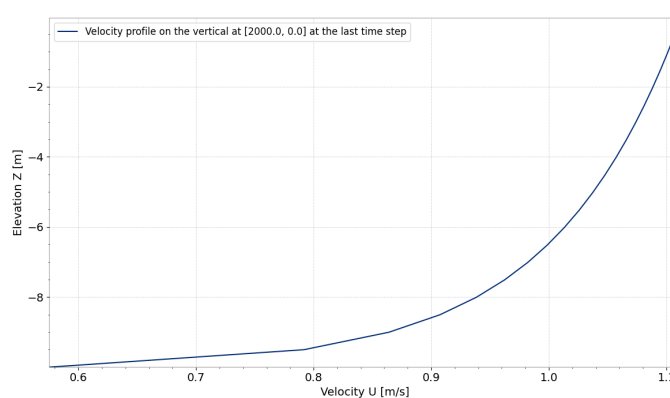


Figure 12.1: Velocity profile comparison

agreement.

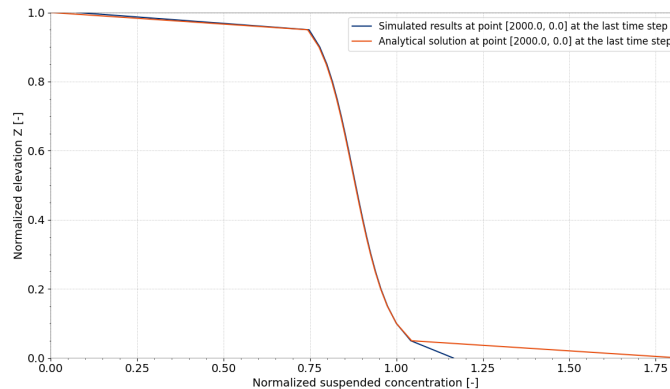


Figure 12.2: Concentration profile comparison

## 12.4 Conclusion

These comparisons with analytical solutions, in hydrodynamics or suspended sediment transport, thoroughly validate the treatment of vertical diffusion and settling velocity in TELEMAC-3D. The mixing length turbulence model of Nezu and Nakagawa and the computation of vertical velocity gradients are also validated.

**12.4.1 Reference**

- [1] HERVOUET J.-M., VILLARET C. Profil de Rouse modifié, une solution analytique pour valider TELEMAC-3D en sédimentologie. EDF-LNHE Report HP-75/04/013/A.

# 13. Sliding

## 13.1 Purpose

The purpose of this test is to show the effect of the two sliding formulations available in GAIA.

## 13.2 Problem setup

The 160 m long and 11 m wide flume is taken from the sandpit test case. The bottom was scaled by factor 10 in order to get higher slopes (see Figure 13.1). All boundaries are closed set and the initial water levels are set constant in order to prevent a flow.

One sediment class with a diameter of 0.1 mm is used. Normal sediment transport is avoided by using Meyer-Peter and Müller formula with a MPM factor of zero. Therefore the bottom evolution origins only from the sliding formulations.

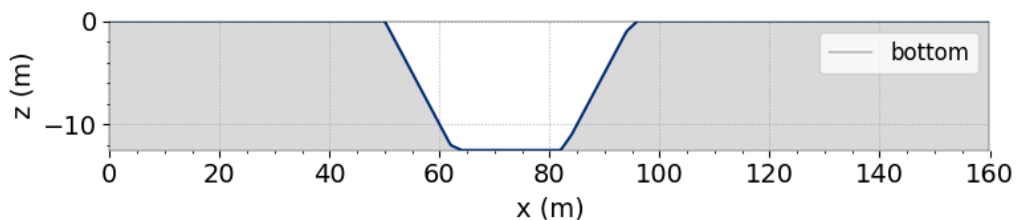


Figure 13.1: Longitudinal section at initial topography.

## 13.3 Numerical setup

Numerical simulations were conducted on an unstructured, triangular finite element mesh with 1600 elements and 819 nodes (Figure 13.2). The simulation started with a constant water level of 2.55 m. The initial water levels are set to 2.55 m. The two sliding formulations (SEDIMENT SLIDE = 1 or 2) are compared using different slope effects (FORMULA FOR SLOPE EFFECT = 1 to 3 and FORMULA FOR DEVIATION = 1 to 3). The angle of repose is set to FRICTION ANGLE OF SEDIMENTS = 20°.

The time step is set to 1 s and the simulation runs for 1000 s in order to reach steady conditions with bottom slopes equals  $\leq 20^\circ$ .

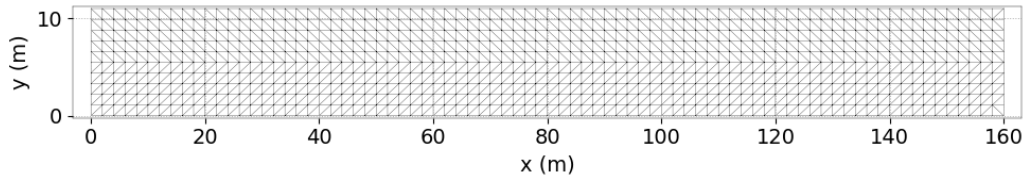


Figure 13.2: Discretization of the flume.

## 13.4 Results

Numerical results of the final bottom using the two sliding formulas *slope smoothing* or *avalanching* are shown in Figure 13.3. The avalanching formula calculates no significant differences in the cross sections as expected. The slope smoothing seems to be influenced by the mesh and creates bottom differences in y-direction.

The comparison between both sliding formulas and the given angle of repose is presented in Figure 13.4 using a longitudinal flume section. It can be seen that with the avalanching formula the angle of repose is reached. With the bottom smoothing formula the final angle is lower than the prescribed angle of repose. Furthermore, as expected different slope and deviation formulas show no influence for none of the sliding formulas.

Figure 13.5 and 13.6 present the bottom evolutions at different time steps for both sliding formulations and Koch and Flokstra slope and deviation formulas. The bottom smoothing sliding formula reaches the steady state much later than the avalanching formula.

With the help of the avalanching formula a fast and grid independent solution to avoid steep slopes can be achieved.

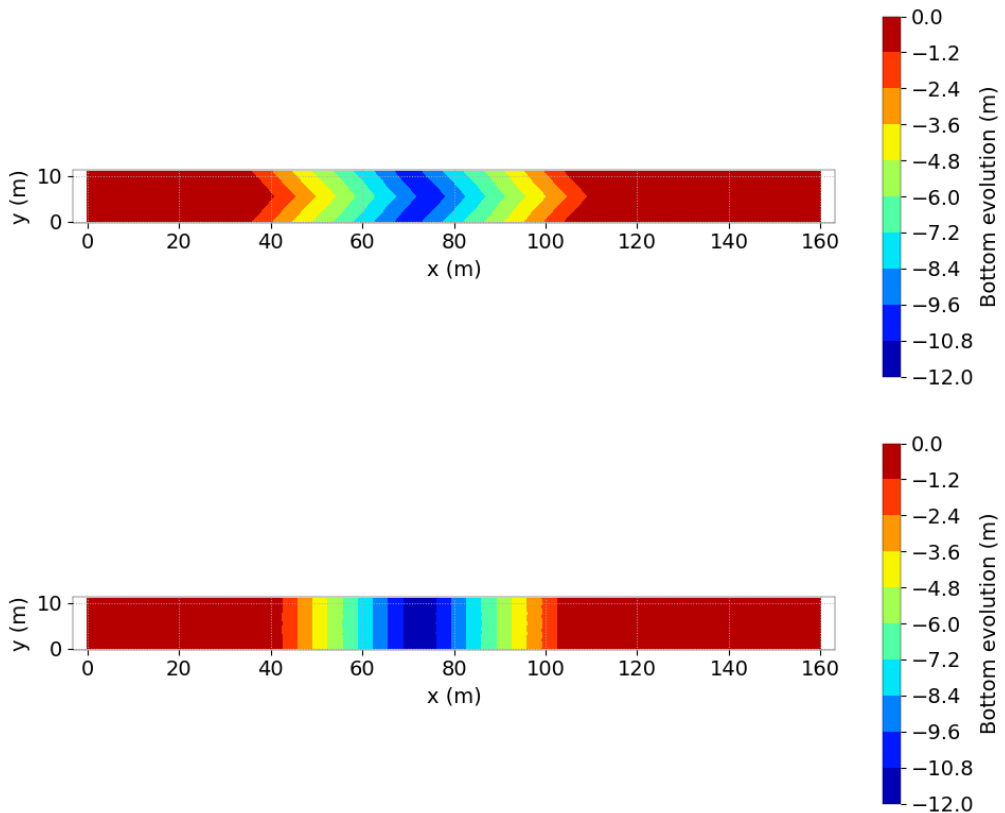


Figure 13.3: Simulated final bottom using slope and deviation effect of Koch and Flokstra with *slope smoothing* sliding formula 1 (top) and with *avalanching* sliding formula 2 (bottom).

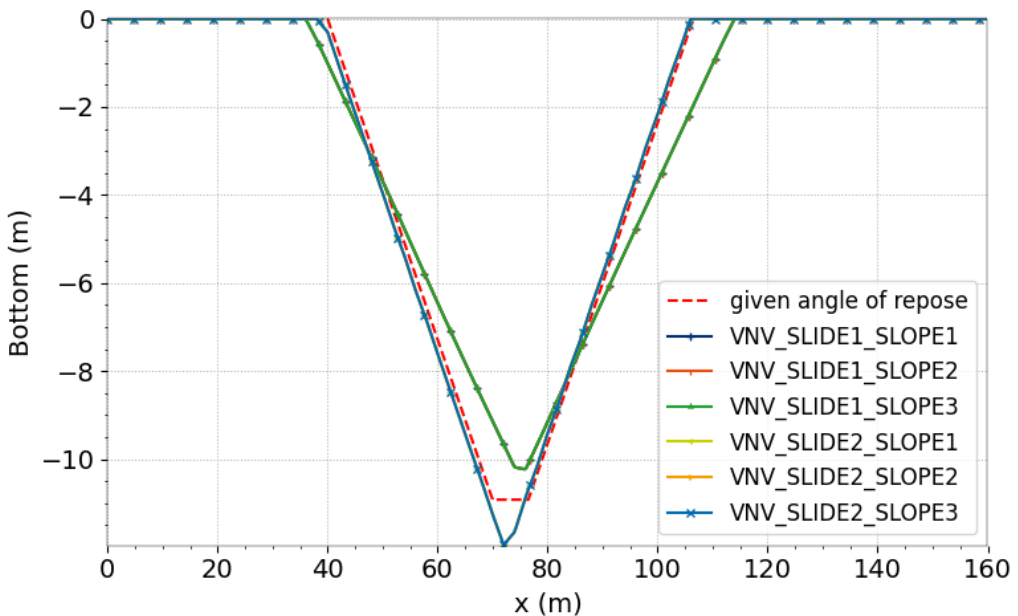


Figure 13.4: Comparison of simulated bottom elevation at a longitudinal flume section for all sliding and slope formulations.

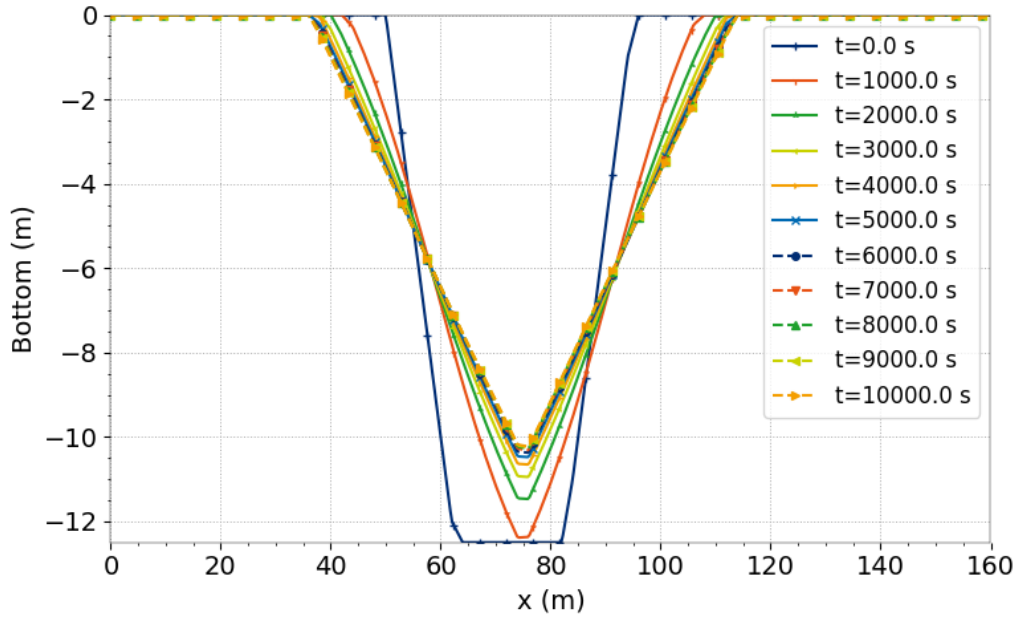


Figure 13.5: Simulated bottom elevation at a longitudinal flume section for the sliding formula 1, slope 1 and different time steps

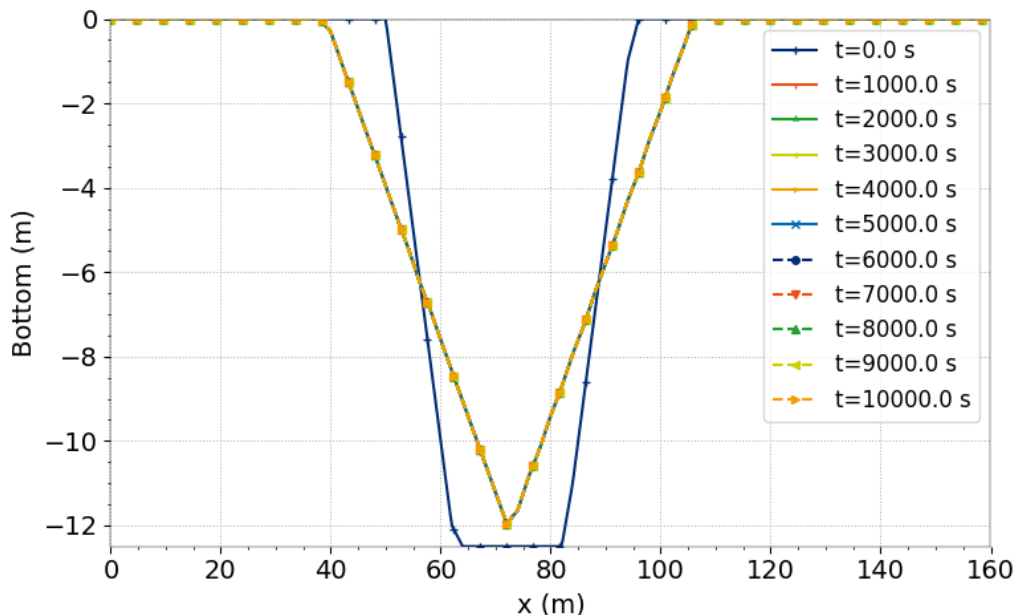


Figure 13.6: Simulated bottom elevation at a longitudinal flume section for the sliding formula 2 and slope 1 and different time steps

## 14. Tidal\_flats-t3d

### 14.1 Purpose

For modelling 3D sediment transport, it is necessary to model the vertical fluxes of the sediment in suspension due to settling and diffusion in addition to the bed exchange fluxes due to erosion and deposition. In shallow tidal areas, the combination of high bed shear stresses and small water volumes can lead to oscillations in the numerical solution, making it inherently difficult to model these vertical processes efficiently and accurately. The objective of this test case is to assess the vertical settling algorithm and diffusion scheme with respect to mass conservation and stability on tidal flats (wetting and drying of mesh elements). It is shown that by choosing the keyword option ADVECTION-DIFFUSION SCHEME WITH SETTLING VELOCITY = 1 the computation can be more efficient and achieves good mass conservation in the situation of tidal flats when considering suspended sediments [1].

### 14.2 Description

In this test case, a large scale tidal flume (50 km long, 5 km wide and 10 m deep) is used, with a 2 m tidal range imposed on the seaward (west) boundary. At the opposite end of the tidal flume, the bed shallows to create a region of wetting and drying. The currents induced by the tide cause sediment on the right hand side of the model to be eroded into suspension. Sediment is therefore in suspension in the area of wetting and drying and erosion and deposition can also occur here. Therefore the simulation is well designed to test the mass conservation of sediment in intertidal areas.

#### 14.2.1 Geometry

##### Model domain

The model domain is rectangular, with a length of 50 km and width of 5km.

##### Mesh

The finite element mesh (Figure 14.1) comprises 4762 triangular elements and 2492 nodes. Element sizes are up to 500 m in the west hand side of the domain and reduce to 80 m near sloping bed area on the right hand side of the model. The vertical discretisation of the model consists of 10 regularly spaced sigma planes.



Figure 14.1: Tidal flats model mesh

### Bathymetry

The bathymetry of the flume is -10 m MSL across most of the domain, with a linear slope on the eastern end of the domain rising from -10 m MSL to +2 m MSL over a distance of 10 km.

#### 14.2.2 Physical parameters

##### Friction

Bed friction is specified using a Nikuradse roughness length of 0.01 m

##### Turbulence

Vertical turbulence is modelled using the mixing length model of Nezu and Nakagawa. Horizontal turbulence, which is less important for this test case, is applied using a constant viscosity of 0.5 m<sup>2</sup>/s for the velocities and 0.01 for the suspended sediment.

##### Sediment

Suspended concentration is initialised to zero throughout the domain. A single bed layer of 10 m thickness (density 500 g/l) is initialised in the right half of the domain. This sediment is too far from the boundary to pass out of the domain in the modelled time frame, therefore boundary fluxes can be ignored in the mass conservation checks.

Erosion is parameterised using a critical shear stress for erosion of 0.01 N/m<sup>2</sup> and a Partheniades erosion rate parameter of 4.0 10-5 kg/m<sup>2</sup>/s. An additional limitation to prevent erosion when the water depth is below a minimum value of 0.1 m is applied.

For settling, a constant settling velocity of 1 mm/s is prescribed.

#### 14.2.3 Initial and Boundary Conditions

##### Initial conditions

Initial conditions are set using a constant elevation of 1 m (i.e. 11 m depth) and velocities are not initialised (i.e. they start at zero). Sediment concentration is initialised to 0. g/L everywhere. A single bed layer of 10 m thickness (density 500 g/l) is initialised in the right half of the model domain. This sediment is too far from the boundary to pass out of the domain in the modelled timeframe, therefore boundary fluxes can be ignored in the mass conservation checks.

##### Boundary conditions

An open boundary is specified at the western end and forced using a sinusoidal tide (1 m amplitude, 0 m MSL mean level, 12 hour period).

Upstream boundary:

- prescribed tidal curve (2 m amplitude, 12 h period)
- zero sediment concentration applied (it is eroded from the bed)

Bottom:

- solid boundary with Nikuradse bed roughness of  $k_s = 0.01$  m

Lateral wall:

- no friction

#### 14.2.4 General parameters

The model was run with a time step of 50 s for a total simulation duration of 86,400 s (24 hours)

#### 14.2.5 Numerical parameters

Advection for velocities and sediment: Scheme 13 (MURD3D\_POS) Option 1 (explicit)

### 14.3 Results

The currents generated due to the tidal boundary create currents which suspend the bed sediment in the model domain (Figure 14.2) at  $t = 22$  hours.

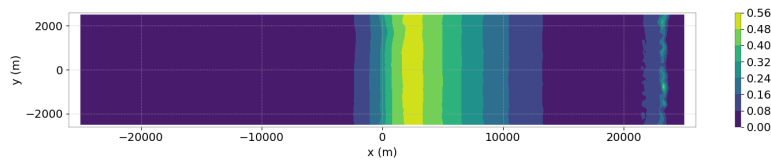


Figure 14.2: Suspended sediment plan view

Figure 14.3 shows a 5.5 km longitudinal section on the slope of the velocity  $U$  at time 22 h. Figure 14.4 shows the suspended concentration for the same longitudinal section.

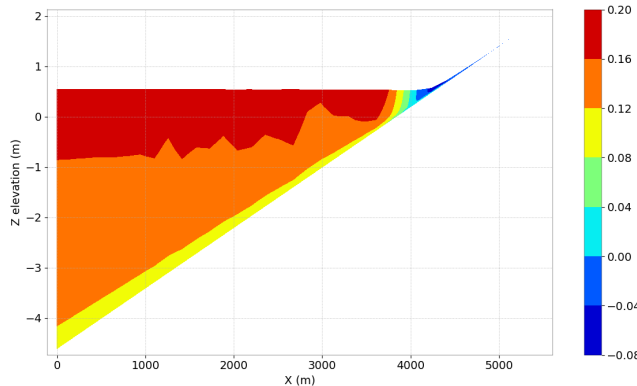


Figure 14.3: Velocity  $U$  section

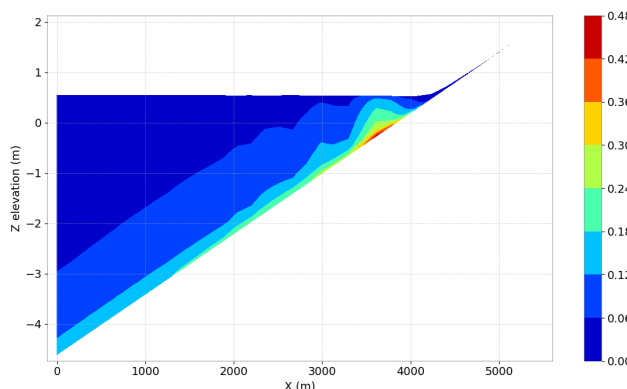


Figure 14.4: Suspended sediment section

Capring of the mass error for suspended sediment for the models run with either SETDEP=0 or SETDEP=1 (Figure 14.5) shows that using SETDEP=1 is marginally better in terms of mass conservation. The model run also runs about twice as quickly due the use of the direct tridiagonal solver method (as opposed to the iterative solver method which requires a high accuracy of convergence).

The bed mass errors are extremely small if using either SETDEP=1 or SETDEP=0 (Figure 14.6). When the mass errors for the suspension and the bed are combined, the plot is almost identical to the mass error for suspension only (Figure 14.7).

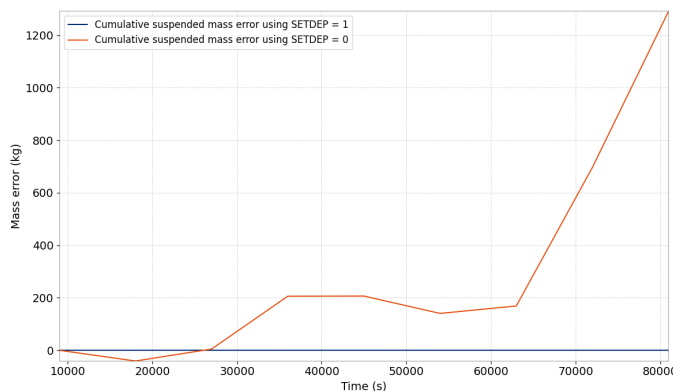


Figure 14.5: Suspended mass error comparison

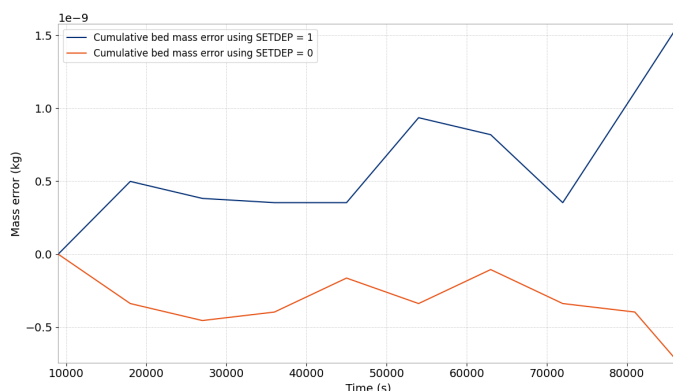


Figure 14.6: Bed mass error comparison

## 14.4 Conclusion

The vertical advection-diffusion scheme (option=1) is found to be remarkably stable and mass conservative even when using relatively large time steps, whereas option=0 necessitates a reduction in the time step and an increase in solver accuracy.

### 14.4.1 Reference

- [1] BENSON T., VILLARET C., KELLY D.M., BAUGH J. (2014) Improvements in 3D sediment transport modelling with application to water quality issues. Proceedings of the 21st Telemac and Mascaret Users Conference. Grenoble, France.

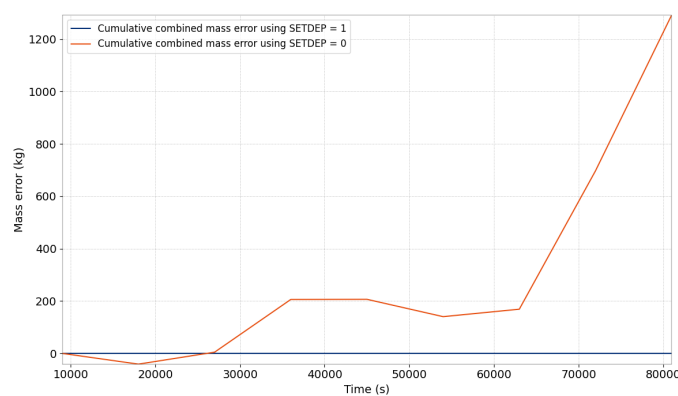


Figure 14.7: Combined mass error comparison

# 15. Turbidity channel

## 15.1 Purpose

The purpose of this case is to demonstrate that TELEMAC-3D coupled with GAIA are able to simulate the plunging of a turbidity current. A schematic reservoir is built and we compare TELEMAC-3D with empirical formulae regarding the location of the plunging point and the vertical velocity profile.

Turbidity currents occur in reservoirs where the density of the incoming flow is significantly different from that of the still water of the lake. This difference of density is mainly due to the concentration of suspended sediments. The capability of a numerical model to reproduce the plunging of a turbidity current depends on the correct simulation of the vertical stratification.

## 15.2 Problem setup

The model is a straight flume, 1000 m long, 10 m wide, with a slope of 0.2%. The upstream discharge is  $2 \text{ m}^3 \text{s}^{-1}$ , a downstream water depth of 1.5 m is prescribed. An upstream sediment concentration is prescribed (50 g/l), the downstream output of sediment is free.

The friction is simulated with a Nikuradse law and a roughness length of 0.01 m.

The initial condition is a stationary flow without sediment simulated with the same hydrodynamic boundary conditions (see Figure 15.1).

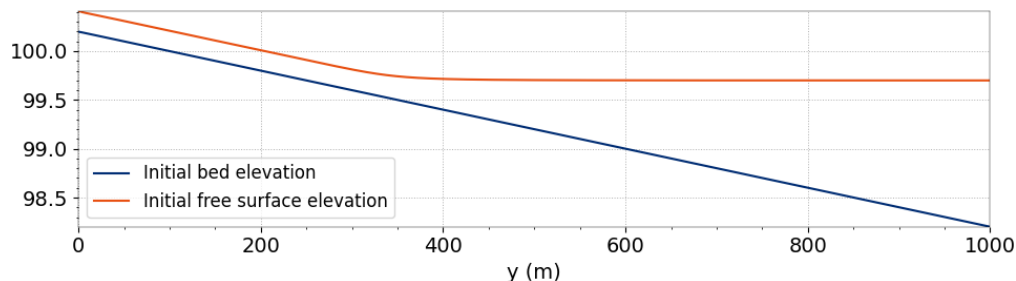


Figure 15.1: Initial condition.

The sediment are cohesive with a settling velocity of 0.1 mm/s. The initial bed does not contain any sediment. Critical shear stresses for deposition and erosion are respectively 0.1 and 1000 Pa.

### 15.3 Numerical setup

Horizontal mesh size is 1 m, 30 vertical layers with constant elevation are used. The vertical mesh between nodes of coordinates (5 ; 10) to (5 ; 50) can be seen on Figure 15.2.

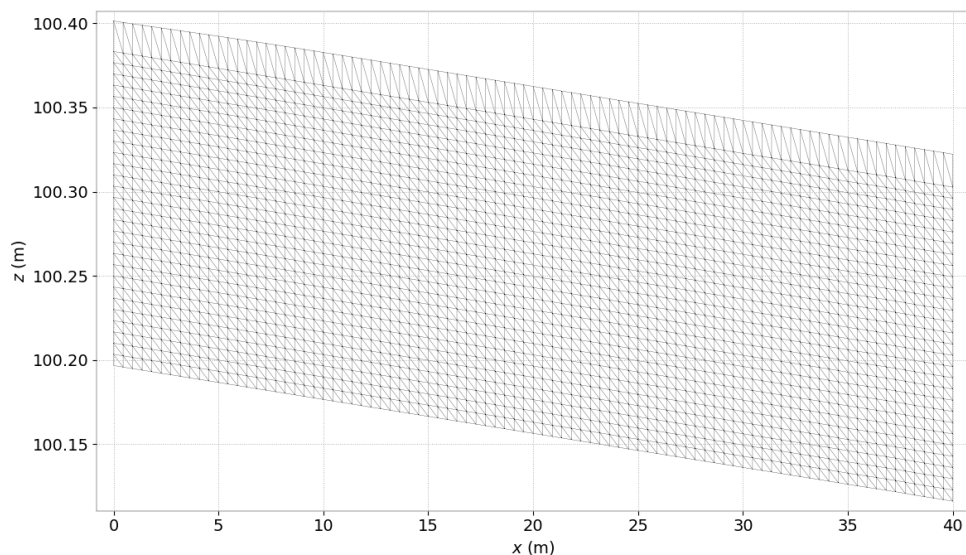


Figure 15.2: Vertical mesh

The time step is set to 0.5 s.

The k- $\varepsilon$  turbulence model has been chosen.

### 15.4 Results

#### 15.4.1 Plunging point

Figure 15.3 shows the concentration in the reservoir after 6000 s. We can compare the location of the simulated plunging point with an empirical assessment.

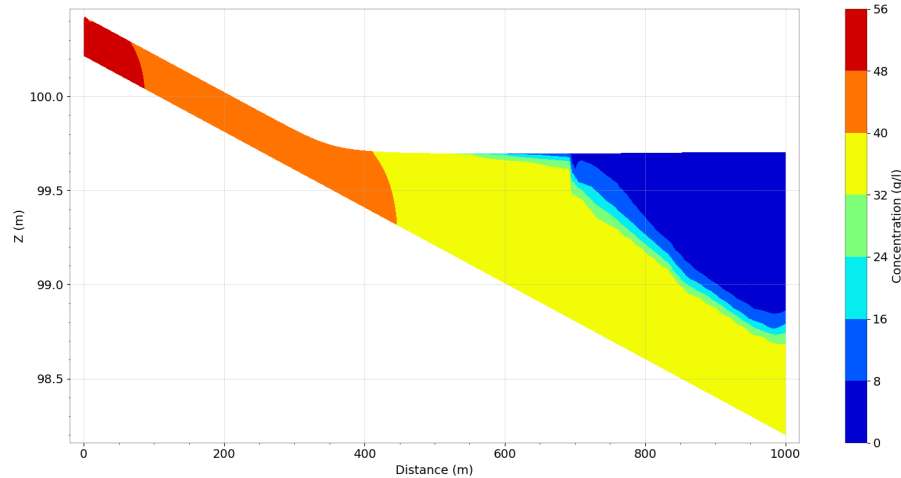


Figure 15.3: Concentration at the final state, slice along the central axis of the channel.

Several empirical and theoretical studies between 1970 and 1990 have established a relationship between upstream flow characteristics and depth,  $H_p$ , at the plunging point [1]. For a straight flume with constant slope, it writes:

$$H_p = K \left( \frac{q_0^2}{\sqrt{g'}} \right)^{1/3} \quad (15.1)$$

Where  $g' = g \frac{\rho - \rho_0}{\rho_0}$ ,  $g$  is the gravity.  $K$  is a coefficient from 1.3 [2] to 1.6 [3].

In the simulation, the plunging point is located at  $y=700$  m. Using the theoretical formula with  $K=1.6$ , we estimate the position of the plunging point at 654 m.

## 15.5 Reference

- Garcia, M. Sedimentation engineering: processes, measurements, modeling, and practice, ASCE, 2008
- Singh, B. & Shah, Plunging phenomenon of density currents in reservoirs, La Houille Blanche, 1971
- Farell, G. & Stefan, H. , Mathematical modelling of plunging reservoir flows, Journal of Hydraulic Research, 1988 , 26 , 525-537

## 16. WC\_BOMC4: experiments of Wilcock and Crowe (2003)

### 16.1 Validation with the experiments of WC-2003

The implementation of the WC-2003 formula is validated with running a model which reproduces two of the experiments of Wilcock and Crowe [21], and comparing the sediment transport rates obtained numerically with applying the formula analytically. To this goal, experiments BOMC2 and BOMC4 are selected, which are characterized by very low and moderate sediment transport rates, respectively. With discretizing the initial GSD into one, two, five and ten size fractions of sediment, the fractional transport rates are computed with Sisyphe for BOMC2 and BOMC4 experiments. The initial GSD has been chosen as the bulk GSD used in the experiments but also as the surface sediment sampled in the end of the experiments [3, 21]. Several methods used for discretizing the GSD have been compared. The recirculation of sediment is considered for each of these experiments. More details on this work can be found in [3].

Here, we show only a single comparison between the analytical results and the numerical results aiming to reproduce experiment BOMC4, where the GSD used in the numerical model corresponds to the bulk sediment and the GSD is discretized into 5 classes of sediment where the fraction volumes content of sediment are initially equal for each size fraction (*i.e.*  $F_{a,i} = 0.2$ ,  $\forall i \in [1 : 5]$ ). Here, the coefficient to calibrate the formula of WC-2003 is set equal to  $\alpha_b = 1$ . The spatially averaged shear velocity obtained at the end of the numerical run ( $\bar{u}_* = 0.084$  m/s) is used as input variable to compute analytically the fractional transport rates.

The simulation is run for short-term simulations of 20 s so that bed topography remains almost unchanged, sorting of sediment is avoided and consequently computed sediment transport rates remain nearly uniform over space. The benchmark source files of this numerical test are available in the folder WC\_BOMC4. The files used to process the numerical results and to compute the averaged fractional transport rates and shear velocity are found in WC\_BOMC4/mean\_qb\_WC\_5CL.py and WC\_BOMC4/mean\_shear\_velocity\_WC\_5CL, respectively. The analytical procedure is available in WC\_BOMC4/Analytical\_model\_WC2003\_BOMC4.xlsx. The comparison between the fractional and total transport rates of sediment obtained analytically and numerically (Tab. 16.1) show that the model of WC-2003 is well implemented in the TMS.

### 16.2 Implementation of sediment recirculation

Laboratory experiments of sediment transport measurement *e.g.* [15, 21, 22] and channel morphodynamics with dunes and bars *e.g.* [5, 9, 11, 12] often rely on the use of sediment recircula-

Table 16.1: Comparison between analytical and numerical results, showing that the formula of WC-2003 is well implemented in the TMS.

Bedload [m <sup>2</sup> /s]	Analytical	Numerical
Total $\bar{q}_{b0}$	$6.77 \cdot 10^{-6}$	$6.78 \cdot 10^{-6}$
$\bar{q}_{b0,1}$	$3.02 \cdot 10^{-6}$	$3.02 \cdot 10^{-6}$
$\bar{q}_{b0,2}$	$2.02 \cdot 10^{-6}$	$2.02 \cdot 10^{-6}$
$\bar{q}_{b0,3}$	$1.19 \cdot 10^{-6}$	$1.19 \cdot 10^{-6}$
$\bar{q}_{b0,4}$	$5.38 \cdot 10^{-7}$	$5.41 \cdot 10^{-7}$
$\bar{q}_{b0,5}$	$7.35 \cdot 10^{-9}$	$7.48 \cdot 10^{-9}$

ing straight flumes. In laboratory, different arrangements can be used for recirculating the water and the sediment [19]. The fundamental differences found between using a sediment feeding flume and sediment recirculating flume has been well documented in the literature [9, 15, 21, 22] and continue to spark debate [1]. For both types of flumes, the upstream water discharge, the downstream water depth and the initial longitudinal bed slope are specified and uniform flow can be maintained [9]. The difference arises when the rate and composition of the input sediment in the feeding experiment differ from the ones of the sediment recirculating experiments, which depend on the downstream exiting sediment. For the sediment recirculating flume, the boundary condition for sediment supply is periodical, so that the recirculating flume has an additional degree of freedom in the system [9].

Using a recirculating flume instead of a feeding flume lead to a different morphodynamic equilibrium when graded sediment is used [1, 9, 15, 21, 22]. Indeed, in the beginning of the experiments with a feeding flume presenting a mild sloping bed, fine sediment is more mobilized than coarser sediment, leading to deposition of coarse sediment upstream and progressive increase of fine sediment content downstream, called *downstream fining* [8, 17, 20]. At the equilibrium, the sediment feeding flume is forced to transport the same rate of coarse sediment than the input rate to follow the equal mobility condition. This equilibrium condition can be only reached by an adjustment of the longitudinal bed slope, which increases in order to increase bed shear stress and mobilize the coarsest sediment.

On the other hand, the results can be strongly different with using a sediment recirculating flume with the same initial conditions and hydraulic boundaries. In the beginning of the experiments, only the fine fraction of sediment is mobilized and migrates out of the flume, before being re-injected upstream. In this case, the coarse sediment can form an immobile layer referred to as lag deposit [9]. As a result, this condition deviates strongly from the hypothesis of equal mobility, with respect to the sediment feeding experiment. The longitudinal equilibrium bed slope is found less modified in comparison with the sediment feeding experiment and the bed shear stress is averaged lower.

The previous analyses outline the importance of dissociating the sediment feeding from the sediment recirculating for long-term morphodynamics studies. Previous numerical studies reproducing [6, 16] Lanzoni's experiments used sediment feeding boundary conditions instead of recirculating sediment. Mendoza *et al.* [13] and Cordier *et al.* [4] considered recirculation of sediment in order to get as close as possible to Lanzoni's laboratory conditions and investigate the long-term morphodynamics of bars with this configuration.

### 16.2.1 Implementation of sediment recirculation in Sisyphe (not in library)

The implementation of sediment recirculation is performed with modifying the subroutine `conlit.f`. The procedure consists on computing the solid transport rates exiting the downstream boundary at the previous time step of computation for each size fraction (here NSICLA=2)

of sediment (lines 40→41 and 61→62), and redistributing the same volume of sediment at each upstream computational node (lines 108→110). This last step requires to specify manually the number of upstream nodes at line 109. In the case where  $t = 0$  s (*i.e.* first time-step), the prescribed fractional transport rates are set equal to 0. In the case where the transport rate is close to the zero machine, we impose a transport rate equal to 0. See the subroutine `user_fortran/conlit.f` for further details.

# 17. Yen

## 17.1 Purpose

The purpose of this test is to assess the ability of GAIA to reproduce the bed evolution in an alluvial channel bend under unsteady-flow conditions. The mechanics of sediment transport in channel bends, frequently appearing in natural rivers, are much more complex than that in straight channels. The complexity is twofold: on the one hand, the sediment transport in a channel bend is subject not only to longitudinal transport, but also to transverse transport and transverse sorting by the secondary flow inherently associated with bends. On the other hand, the unsteadiness of flow in natural rivers certainly has some effects on the structure of the flow field, thereby affecting the motion of sediment particles.

This test is the experimental setup (RUN 4) proposed by Yen and Lee (1995). In this case, the bed evolution of a 180° channel bend with an initial flat bottom is computed for a triangular-shaped 300 min. hydrograph. Numerical results are validated by measured contours of bed evolution after at the end of the experiment and by measured bottom elevations at two different cross sections (90° and 180°). This validation case can be performed for uniform or graded sediment distribution. There are several cases in this example. With graded sediments all implemented bedload formulas (except one because it needs waves) and hiding formulas are tested. With uniform sediments all implemented slope formulations are tested. Since only the sediment diameters are variable, the results with 1 class or with 5 classes can all be compared to the experimental data. An additional test was added to test the keyword SPINUP TIME FOR BED UPDATING. In this test, a run with bed load and suspended load is executed, with a hydrodynamic spinup time of 12 minutes.

## 17.2 Problem setup

The flume consists of a straight section of 11.5 m long, a 180° bend of 4.0 m radius and a downstream straight section of 11.5 m long, with a constant slope in flow direction equal to 0.002. The width of the flume channel is 1.0 m. A triangular-shaped inflow hydrograph with an initial discharge of  $Q = 0.02 \text{ m}^3/\text{s}$ , a water depth at the outflow of  $h = 0.0544 \text{ m}$  and a peak discharge of equal to  $0.053 \text{ m}^3/\text{s}$  (water depth  $h = 0.103 \text{ m}$ ) at  $T = 100 \text{ min}$  is used, see Figure 17.1. After  $T = 100 \text{ min}$ , the inflow discharge is reduced linearly until it reached the initial values at the end of the experiment ( $T = 300 \text{ min}$ ).

The sediment is characterized by a median diameter of  $D_{50} = 1 \text{ mm}$ . This value is used for the case uniform sediment. For the case graded sediment, five sediment classes with diameters

$D = 0.31, 0.64, 1.03, 1.69$  and  $3.36\text{ mm}$  are chosen to reproduce the sediment distribution of the experiment. For this case, an initial distribution of 20% for each class is adopted. All implemented bedload transport formulas are tested as well as all slope effect formulas. The secondary currents correction are accounted for this test. The default value of  $\alpha = 1$  is used for the secondary currents parameter, therefore the Engelund parameter  $A = 7$ . For the case graded sediment, two vertical sediment layers with a total thickness equal to 20 cm are assumed.

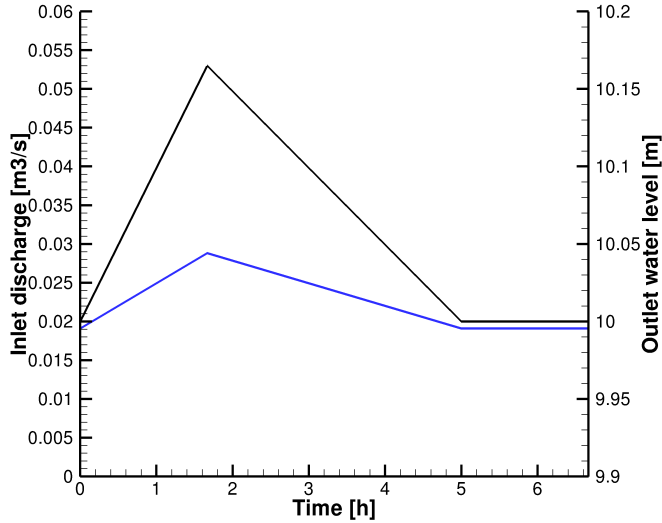


Figure 17.1: Triangular-shaped hydrograph.

A friction closure relationship, based on the Nikuradse roughness length is adopted to account for the bed resistance. For this case,  $k_s = 3.5\text{ mm}$  ( $\approx 3 \times D_{50}$ ) and the Elder model is specified to parameterize the turbulent eddy viscosity. The critical Shields parameter is set at 0.047 and the bed porosity is 0.375.

### 17.3 Numerical setup

Numerical simulations were conducted on an unstructured, triangular finite element mesh with 3230 elements and 1799 nodes and a mean grid size of the order of 0.20 m (Figure 17.2). As initial condition, a fully developed (stationary) flow with a constant water-depth  $h = 0.0544\text{m}$  and discharge  $0.02\text{ m}^3/\text{s}$  is imposed and the bottom has a constant slope in flow direction equal to 0.002.

The time step is set to 0.5 s. For a mean velocity in the range  $[0.37 - 0.53]\text{ m/s}$  and a mean grid size of the order of 0.2 m, the mean Courant number varies between 0.6 and 1.3.

For a daily validation the duration is limited to 2 hours instead of 5 hours.

### 17.4 Results

The measurements were done after 5 hours but for the daily validation the simulation duration was decreased to 2 hours. For a proper comparison the simulation duration must be increased to 5 hours as well. Numerical results of the normalized bed evolution are shown in comparison with measurements. Morphological changes exhibit the expected patterns of erosion and sedimentation at the channel bend, with the presence of a point bar along the inner-bank and a deeper channel along the outer-bank of the bend. The computed bed changes are in agreement

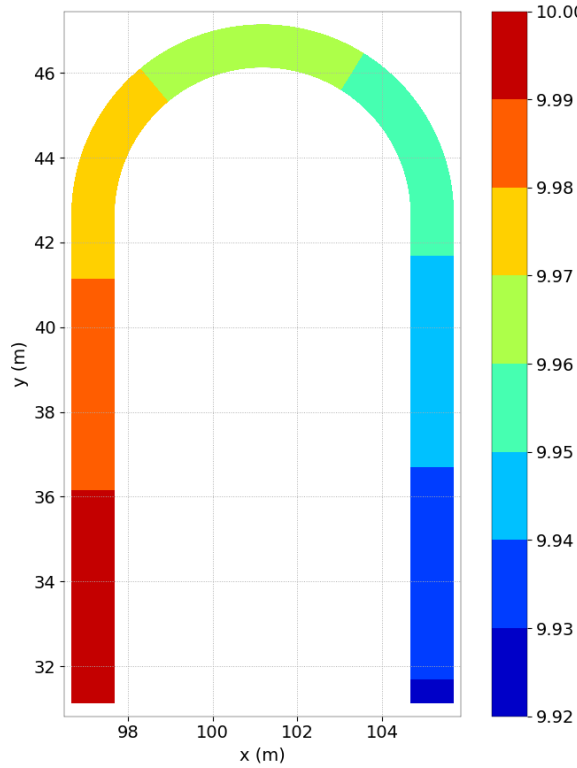


Figure 17.2: Simulation grid and initial bottom.

with the measured data. Without accounting for the secondary flow effect, one cannot obtain such reasonable results. The subsequent Figures, from 17.3 to 17.7 show the most up to date results with all tested configurations with GAIA.

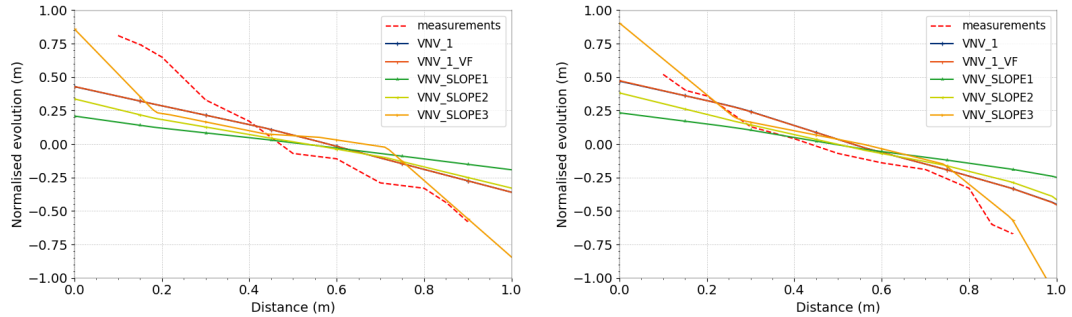


Figure 17.3: Comparison of simulated and measured normalised bed evolution at cross sections 90° (left) and 180° (right), with uniform sediment and the Engelund-Hansen & Chollet-Cunge formula for bedload using Finite Elements (vnv 1) and Finite Volumes (vnv 1 vf) and Meyer-Peter Müller formula with 3 different slope effect formulas (vnv slope1, vnv slope2, vnv slope3).

## 17.5 References

Yen, C. and Lee, K.T. (1995) *Bed Topography and Sediment Sorting in Channel Bend with Unsteady Flow*. Journal of Hydraulic Engineering, Vol.121, No. 8.

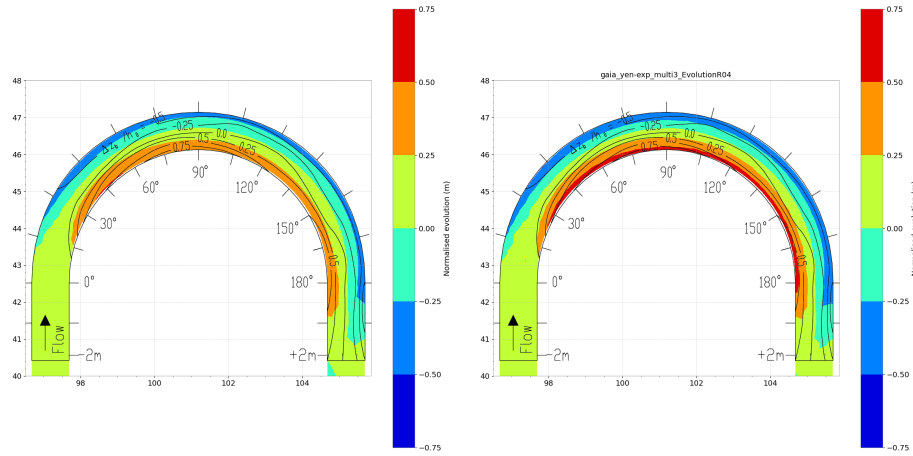


Figure 17.4: Comparison of simulated (coloured) and measured (black contour lines) normalised bed evolution (top) with one sediment class and the Engelund-Hansen & Chollet-Cunge formula for bedload with uniform sediments (left) and with 5 sediment classes (right).

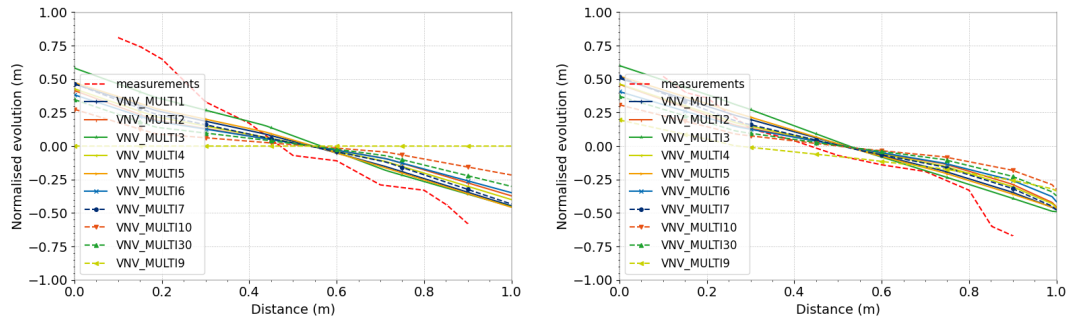


Figure 17.5: Comparison of simulated normalised bed evolution at cross sections 90° (left) and 180° (right), with five sediment classes and different bedload formulas (multi1-multi10).

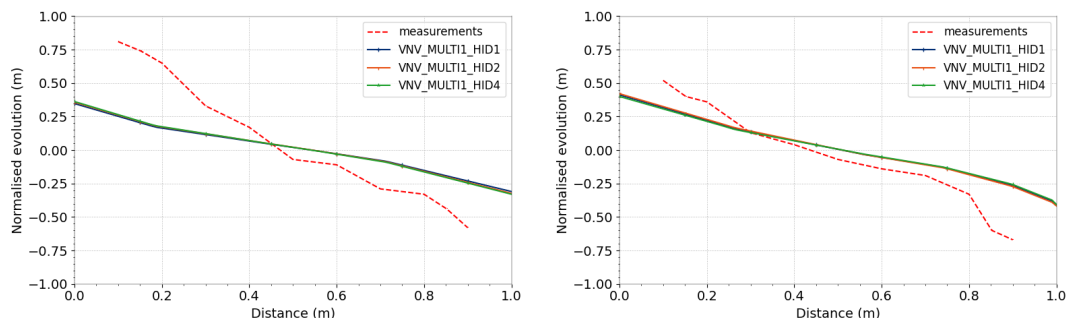


Figure 17.6: Comparison of simulated normalised bed evolution at cross sections 90° (left) and 180° (right), with five sediment classes and different Meyer-Peter und Müller bed load formula and different hiding formulas (multi1 hid1 - multi1 hid4).

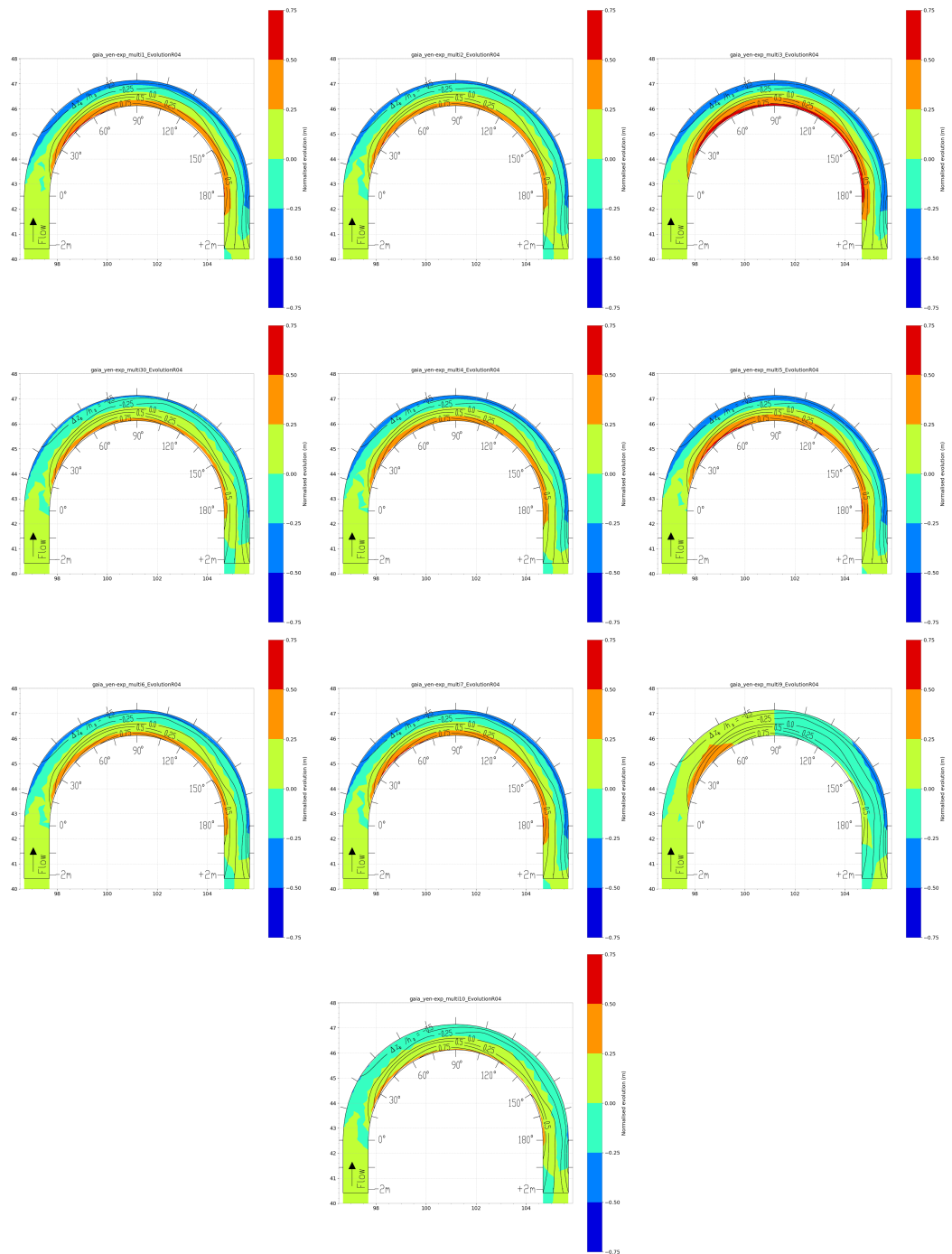


Figure 17.7: Comparison of simulated (coloured) and measured (black contour lines) normalised bed evolution with five sediment classes and different bedload formulas (multi1-multi10).

- [1] R Bettess. Discussion of sediment feed and recirculating flumes: Fundamental difference by gary parker and peter r. wilcock. *Journal of Hydraulic Engineering*, 121(3):292–294, 1995.
- [2] WA Breugem, E Fonias, L Wang, and A Bolle. Tel2tom: coupling telemac2d and tomawac on arbitrary meshes. In *XXVIthTELEMAC-MASCARET User Conference*. XXVIth TELEMAC-MASCARET User Conference, October 2019.
- [3] F. Cordier, P. Tassi, N. Claude, A. Crosato, S. Rodrigues, and D. Pham Van Bang. Numerical modelling of graded sediment transport based on the experiments of wilcock and crowe (2003). In *XXIIIrd TELEMAC-MASCARET User Conference Proceedings*, 2016. URL <http://www.opentelemac.org/index.php/2016>.
- [4] F. Cordier, P. Tassi, N. Claude, A. Crosato, S. Rodrigues, and D. Pham Van Bang. Influence of sediment size heterogeneity on free and hybrid alternate bar morphodynamics. *Water Resources Research*, Under revision, 2018.
- [5] Alessandra Crosato, Frehiwot Beidmariam Desta, John Cornelisse, Filip Schuurman, and Wim S. J. Uijttewaal. Experimental and numerical findings on the long-term evolution of migrating alternate bars in alluvial channels. *Water Resources Research*, 48(6):1–14, 2012. ISSN 1944-7973. doi: 10.1029/2011WR011320. URL <http://dx.doi.org/10.1029/2011WR011320.W06524>.
- [6] A. Defina. Numerical experiments on bar growth. *Water Resources Research*, 39(4), 2003.
- [7] Arthur Günter. *Die kritische mittlere Sohlenschubspannung bei Geschiebemischungen unter Berücksichtigung der Deckschichtbildung und der turbulenzbedingten Sohlenschubspannungsschwankungen*. PhD thesis, ETH Zurich, 1971.
- [8] Trevor B Hoey and Rob Ferguson. Numerical simulation of downstream fining by selective transport in gravel bed rivers: Model development and illustration. *Water Resources Research*, 30(7):2251–2260, 1994.
- [9] MG Kleinhans. Experimental dune trough scour in sediment mixtures. *Marine Sandwave and RIver Dune Dynamics*, 2004.
- [10] Ethan J. Kubatko and Joannes J. Westerink. Exact discontinuous solutions of exner's bed evolution model: Simple theory for sediment bores. *Journal of Hydraulic Engineering*, 133(3):305–311, 2007.
- [11] Stefano Lanzoni. Experiments on bar formation in a straight flume 1. uniform sediment. *Water Resources Research*, 36(11):3337–3349, 2000.

- [12] Stefano Lanzoni. Experiments on bar formation in a straight flume: 2. graded sediment. *Water Resources Research*, 36(11):3351–3363, 2000.
- [13] Alejandro Mendoza, Jorge D Abad, Eddy J Langendoen, Dongchen Wang, Pablo Tassi, and Kamal El Kadi Abderrezak. Effect of sediment transport boundary conditions on the numerical modeling of bed morphodynamics. *Journal of Hydraulic Engineering*, 143(4): , 2016.
- [14] Gary Parker and Peter C. Klingeman. On why gravel bed streams are paved. *Water Resources Research*, 18(5):1409–1423, 1982. doi: <https://doi.org/10.1029/WR018i005p01409>. URL <https://agupubs.onlinelibrary.wiley.com/doi/abs/10.1029/WR018i005p01409>.
- [15] Gary Parker and Peter R Wilcock. Sediment feed and recirculating flumes: Fundamental difference. *Journal of Hydraulic Engineering*, 119(11):1192–1204, 1993.
- [16] Honglu Qian, Zhixian Cao, Huaihan Liu, and Gareth Pender. Numerical modelling of alternate bar formation, development and sediment sorting in straight channels. *Earth Surface Processes and Landforms*, 607:613–622, 2016. ISSN 1096-9837. doi: 10.1002/esp.3988. URL <http://dx.doi.org/10.1002/esp.3988>. ESP-15-0409.R2.
- [17] Rebecca Seal, Chris Paola, Gary Parker, John B Southard, and Peter R Wilcock. Experiments on downstream fining of gravel: I. narrow-channel runs. *Journal of Hydraulic Engineering*, 123(10):874–884, 1997.
- [18] JP Soni. Laboratory study of aggradation in alluvial channels. *Journal of Hydrology*, 49 (1-2):87–106, 1981.
- [19] John Southard. *12.090 Introduction to Fluid Motions, Sediment Transport, and Current-Generated Sedimentary Structures*. Fall 2006. Massachusetts Institute of Technology: MIT OpenCourseWare. URL <https://ocw.mit.edu>.
- [20] Carlos M Toro-Escobar, Chris Paola, Gary Parker, Peter R Wilcock, and John B Southard. Experiments on downstream fining of gravel. ii: Wide and sandy runs. *Journal of Hydraulic Engineering*, 126(3):198–208, 2000.
- [21] Peter R Wilcock and Joanna C Crowe. Surface-based transport model for mixed-size sediment. *Journal of Hydraulic Engineering*, 129(2):120–128, 2003.
- [22] Peter R Wilcock and Brian W McArdell. Surface-based fractional transport rates: Mobilization thresholds and partial transport of a sand-gravel sediment. *Water Resources Research*, 29(4):1297–1312, 1993.